Effect of miR-582-5p modulated cancer-associated fibroblasts on vulvar cancer cells

Rezan Erman

This thesis is submitted in partial fulfilment of the requirements for the degree of Master in Biomedical Sciences

Department of Biomedicine

University of Bergen

Spring 2022

Acknowledgements

I would like to thank my main supervisor Harsh Nitin Dongre for taking out time, being supportive and patient. I would also like to thank my co-supervisor Himalaya Parajuli for being helpful and available. A big thank you to Professor Daniela Elena Costea for welcoming me into her research group and always being very inclusive. Lastly thank you to everyone else in the group that would always help me whenever there was something I was wondering about or needed help with or if there was something I could not find.

Table of contents

Summary

Cancer-associated fibroblasts (CAFs) have been shown to promote carcinogenesis in many cancers including vulva squamous cell carcinomas (VSCC). In addition, deregulation of micro-RNAs (miRNAs) in CAFs are known to affect the various cancer hallmarks by either downregulating tumor suppressor oncogenes or increasing the expression of oncogenes. MiR-582-5p is reported to increase tumorigenesis in non-small cell lung carcinomas whereas it decreases cancer progression in colorectal carcinomas. However, its role in VSCC is not known. This study aimed to investigate miR-582-5p dysregulation in CAFs in both human papillomavirus (HPV) E6E7 positive and negative VSCC, and its effects on their phenotype and invasion of adjacent VSCC cells. Gene expression of miR-582-5p was first investigated in VSCC-derived CAFs (n = 5) isolated from fresh tumor biopsies. MiR-582-5p mimics and inhibitors were used to functionally investigate the role of miR-582 on CAF phenotype and the resulting change in their ability to support vulva SCC invasion. Expression of miR-582-5p showed marked heterogeneity in the cultured fibroblasts. Increased miR-582-5p expression enhanced CAFs' motility and colony formation ability, but did not increase invasion of suprajacent vulva SCC cells, while its inhibition resulted in the opposite outcome. There was not a significant difference in miR-582-5p modulated vulva-cancer-associated fibroblast influence on HPV positive compared to HPV-negative vulva squamous cell carcinoma. Despite its heterogeneous expression, miR-582-5p in VSCC-derived CAFs exhibits a tumor-promoting function.

1. Introduction

1.1 Vulvar cancer

Vulvar cancer can arise in any parts of the vulva, which consists of the labia majora, labia minora, vaginal introitus, clitoral hood, paraurethral Skene glands, and posteriorly, the Bartholin's glands (Puppo, 2013). Vulvar cancer is a rare form of cancer and represents about 4% of all cancers in the female genital tract. There are several histological subtypes of vulvar cancer such as squamous cell carcinoma (VSCC), adenocarcinoma, sarcoma, melanoma, and verrucous carcinoma, but by far the most common cancer type (~90%) in the vulva is VSCC. VSCC is a stepwise process from normal tissue to hyperplastic, dysplastic, carcinoma *in situ*, and eventually to invasive carcinoma (Xing & Fadare, 2021). Squamous cells are present in the lining (epithelial layer) of the vulva and they have a protective function and are important to the shape of the organ. As these cells mature, they gradually get pushed out from the basal layer and adopt a fish scale-like morphology. Vulvar squamous cell carcinoma (VSCC) comprises transformed squamous cells. In most cases, VSCC develops from the basal layer of the epithelium. A lot of cancer risk factors are shared amongst the different forms of cancer, but for VSCC, in addition to the common ones, there is also the human papilloma virus (HPV) as a potent risk factor (Lindell et al., 2010).

Although rare, it is an increasing health risk to women worldwide. In Norway, over the period of 1961-2010, the incidence has increased 2.5-fold with an incidence of 4.66 per 100000 women per year in 2012. The increase in incidence is greatest among women younger than 60 (Meltzer-Gunnes et al., 2017).

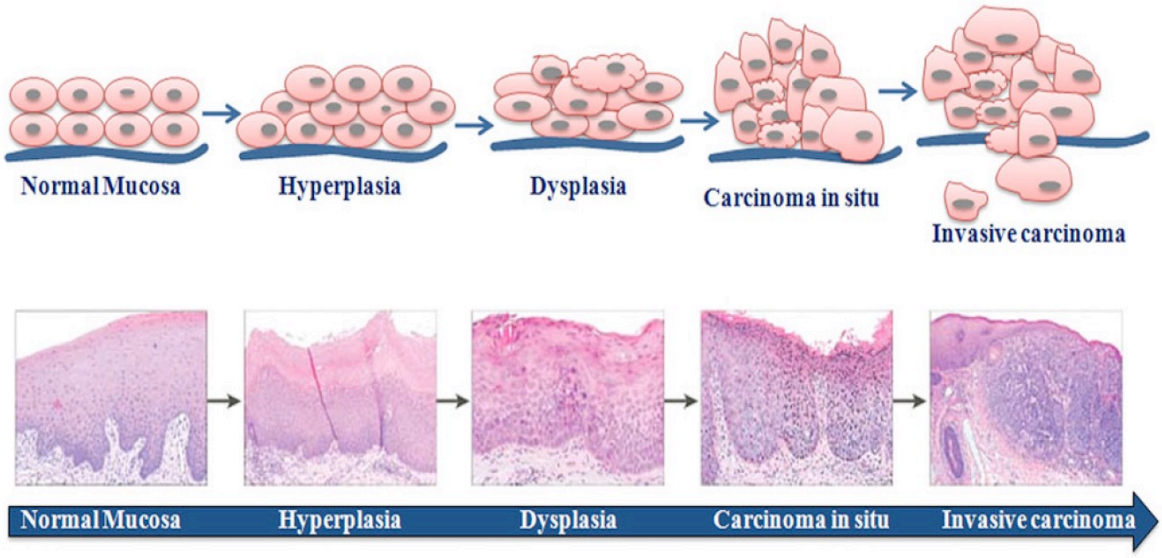

Figure 1. Stepwise progression of vulvar squamous cell carcinoma. Adapted from (Shah et al., 2011).

1.2 Human papilloma virus

Human papillomavirus (HPV) is a group of double-stranded-DNA viruses with over 200 different viruses, and it is the world's most common sexually transmittable infection (Kombe Kombe et al., 2021). This virus targets squamous cells of the epithelium. The viral replication cycle is dependent on the differentiation of squamous cells, and it takes place gradually, as the squamous cells mature. The viral life cycle is complete when the squamous cell reaches the outer layer of the epithelium, which is when the cell is in the release phase of the viral replication. Infection with HPV is considered a risk factor for VSCC, with different HPV viruses having different risks of inducing cancer. Those involved in carcinogenesis were called high risk HPV (hrHPV). A study done in Sweden in 2010 found 31% of VSCCs to be HPV positive (Lindell et al., 2010). A 2018 review (Zhang et al., 2018) of both Asian and Caucasian populations found 34% of all VSCC to be HPV positive; meanwhile, a 2021 review (Kombe Kombe et al., 2021) on HPV epidemiology estimated the HPV prevalence in women in Europe to be 14.2 percent, showing a correlation between HPV infection and VSCC development.

1.2.1 HPV and carcinogenesis

HPV-independent and HPV-dependent VSCC show different pathological pathways of carcinogenesis. A part of the carcinogenic pathway for HPV-dependent VSCC is through to be the immortalization that occurs during the viral transformation, due to two viral genes that are introduced into the squamous cells. One of these is the early gene 6 (E6) gene which inhibits apoptosis by inhibiting the p53 tumor suppressor. And the other is the early gene 7 (E7) gene which increases the proliferation of the cell through inhibition of the retina blastoma protein. These two changes ar enough to immortalize the cell, which then can lead to genomic instability. This genomic instability is thought to drive the transformation of the cells into cancerous cells (Wang et al., 2018). Genomic studies have shown that in HPV-positive cancers, these two genes are consistently maintained; meanwhile, other parts of the viral genome are either disturbed or altogether removed post-cancer transformation (Münger et al., 2004).

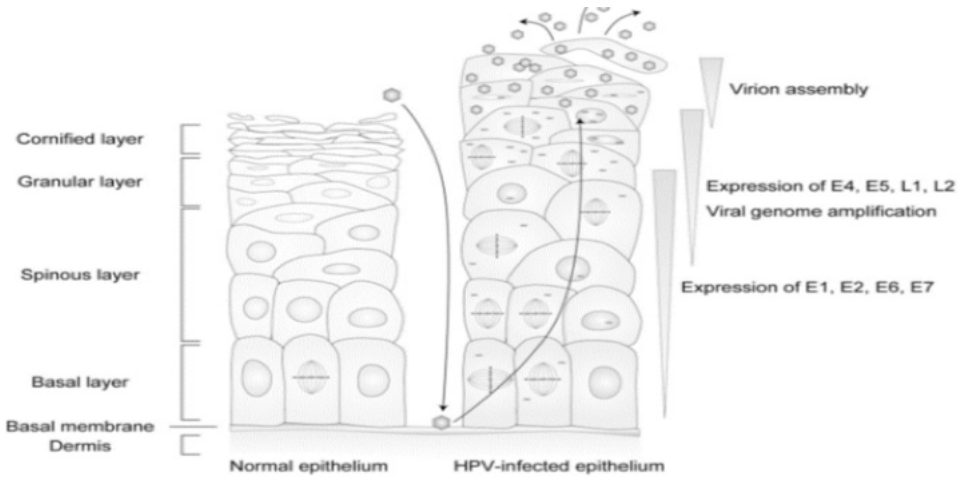

Figure 2. Stepwise viral transformation of squamous cells from hrHPV virus (Moody et al., Nat rev can, 2010).

1.3 Tumor microenvironment

A tumor is a complex tissue, containing in addition to malignant cells nonmalignant cells such as fibroblasts, nerves, blood and lymph vessels, immune cells, fat cells,

soluble growth factors and cytokines, metabolites, and extracellular matrix (ECM), all of these comprise the tumor microenvironment (TME).

Increasing evidence has shown the TME's importance in cancer, causing a shift in research from a cancer centric to TME-inclusive research (Dongre et al., 2020; Jin & Jin, 2020). The TME is thought to be vital to carcinoma's ability to resist therapy, grow, invade, induce angiogenesis and metastasize (Jin & Jin, 2020). Because of this, there has been much research on active components that can target the tumor stroma. It is a common thought that oncogenic mutations initiate carcinogenesis, and then the TME and the cancer cell develop alongside one another where the cancer cells recruit, shape, and train the non-malignant cells; the result is communication and dependency on the nonmalignant stromal cells for the cancer cells. (D'Arcangelo et al., 2020). Studies have also shown that abnormal tissue states such as chronic inflammation can initiate and drive tumorigenesis through epigenetic changes, indicating stroma's importance in cancer (Mantovani et al., 2008; Todoric & Karin, 2019). This explains why chronic inflammation is such a prominent risk factor for cancer. In the TME, fibroblasts are of particular interest because of their intrinsic ability to remodel ECM and promote an inflammatory tissue state by releasing cancer-promoting cytokines.

1.3.1 Fibroblasts

Fibroblasts are stromal cells with migratory capabilities originating from the mesoderm and found in the mesenchyme/connective tissue, such that they are present in virtually all tissue. Fibroblasts have a central role in tissue homeostasis in their quiescent state, as they regulate ECM structure (Costea et al., 2013). Fibroblasts can also be activated by either soluble factors such as TGFb or mechanical forces into myofibroblasts. Myofibroblasts are more secretory, motile and contractile, express a-smooth muscle actin (aSMA), and transiently take part in tissue repair during wound healing and acute inflammation by secreting collagen-rich ECM and releasing inflammatory cytokines that promote proliferation, angiogenesis, and immune cell recruitment (Lemons et al., 2010). During chronic inflammation, they take on an

aberrant stimulatory role by being constantly active; this leads to a cancer-promoting pathological tissue state through hardening of tissue (ECM remodeling) and continuous promotion of angiogenesis, proliferation, and overall proliferation with subsequent genomic instability (Kendall & Feghali-Bostwick, 2014). Already in 1986, Dvorak (Dvorak, 1986) hypothesized tumors to be “wounds that never heal” and further stated that “an appreciation of tumor stroma is essential to understand the biology of tumor growth”. Consistent with that is the chronic inflammatory-like tissue state in tumors, and likewise, aberrant stimulated fibroblasts are also seen in tumors and are called cancer-associated fibroblasts (CAFs). These CAFs are considered to be in a permanent state of activation because they keep this phenotypic change even when taken out of the TME and are grown *in vitro.*

1.3.2 Cancer-associated fibroblasts

Studies have shown that fibroblasts present in the TME are phenotypically unique and different from normal fibroblasts (NFs), indicating that cancer cells and the TME induce stable changes in NFs. There is also heterogeneity amongst the CAFs, with some being thought to be cancer-supporting and others cancer-suppressing (Öhlund et al., 2014). The general phenotype of the CAFs found in the TME much more resembles that of the activated fibroblast both in morphology and phenotype - the myofibroblast found in wounds or in inflamed tissue (Sahai et al., 2020). As mentioned earlier, myofibroblasts release cytokines, chemokines, and growth-promoting factors (Liu et al., 2016). Because of this permanent change in the CAFs induced by the TME, there has been interest in research trying to reverse this activation.

An example of such attempts is the use of the patented anti-cancer compound Minnelide™ in 2018. Through conditioned medium (CM) and cancer assays, the authors of the study showed evidence that the Minnelide™ reversed CAF into a more quiescent state more resembling to that of a NF (Dauer et al., 2018). The dependency of cancer cells on CAFs has been demonstrated in several studies. For VSCC, in 2019, Dongre et.al. established a novel vulvar cancer cell line that exhibited much

greater invasive potential when vulvar CAFs (VCAFs) were present versus when they were not, suggesting that the invasive phenotype in the VSCC was TME dependent (Dongre et al., 2019).

1.3.3 Stromal cell secretome

A cell's secretome comprises anything that a cell secretes. The cells in the TME reciprocally interact with one another, especially with the cancer cells. This communication and crosstalk happens mainly through the cell's secretomes; because of this, the effect of the TME can be looked at by exposing cancer cells to non-malignant TME cell secretomes and then using various assays to look at the impact of the secretome. The most common way of creating cell secretomes in the laboratory is by letting the cells grow in a medium and then collecting this medium after a time interval; this medium containing all that the cells have secreted during that period of time is called conditioned medium (CM).

1.4 Micro RNAs (miRNAs)

MiRNAs are 18-24 nucleotide long single-stranded RNAs that are not translated. They regulate genes post-transcriptionally and do so by binding to the mRNA (Zhu et al., 2021). They are mostly known for repression of translation and they perform this by binding to mRNA to slow down or hinder translation and induce the breakdown of the specific mRNA. Studies have shown evidence that miRNAs also can increase gene expression. A 2008 study showed that miRNA-373 has a complementary sequence on the promoter region of the mRNA of E-Cadherin. Transfection of cells with miRNA-373 was shown to increase the expression of E-Cadherin (Place Robert et al., 2008).

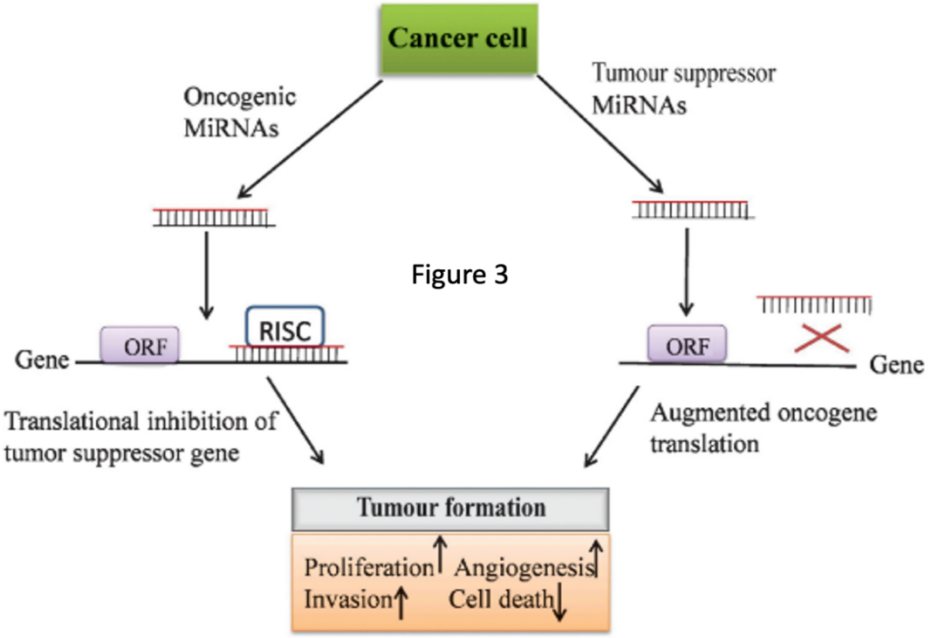

Figure 3 shows how miRNAs can promote tumor formation (Ahmad et al., Indian J Med Res,2013).

1.4.1 MiRNAs role in cancer cells

Studies have shown heavy deregulation of miRNAs in cancer (Iorio & Croce, 2012) (Croce, 2009), either through overexpression or the virtual deletion of certain miRNAs. This deregulation of miRNAs affects the various cancer hallmarks by either downregulating miRNAs that inhibit oncogenes, increasing the expression of various miRNAs that inhibit tumor suppressors, or through an increased expression of miRNAs that increase of expression of oncogenes (Peng & Croce, 2016). A single miRNA will have many target genes, which is seen in how different expression levels of the same miRNA affect different cancer types differently (Pal et al., 2015). In addition, miRNAs can target various transcription factors like Sox2 or Oct4 that can activate the stem cell program in cells. This program can be activated in cancer cells, which transforms the cells into cancer stem cells (CSC) (Xu et al., 2009). Furthermore, an increase in stemness in solid cancer cells that grow normally attached on plastic gives the cells the ability to grow in a matrix, without attachment

to a solid substrate, and to form spheroids. Also, a connection between CSCs in TME and a lack of immune cells was observed in a 2019 study (Miranda et al., 2019). This study brought some evidence for understanding the regulatory network of stem cell marker Oct3/4 via miRNAs in cells, but the role of miRNA is still largely unknown (Müller et al., 2016) (Miranda et al., 2019)

In various cancers, studies have shown both negative and positive prognostic correlations between clinical data and up- or down-regulation of the same miRNAs; this shows how context-based miRNAs are. For example, a 2016 study showed evidence of miRNA-582-5p promoting colorectal cancer by inducing proliferation through upregulation of adenomatous polyposis coli protein (Shu et al., 2016). Later, a 2021 study showed miRNA-582-5p to suppress cell growth and tumorigenesis through inhibition of the expression of oncogenes like YAP, AKT3, NOTCH1, and MAP3K2 in non-small cell lung cancer (Zhu et al., 2021).

2. Aim and objectives

The aim of this study was to decipher the role of miR-582-5p modulated vulvar CAFs on HPV-negative and HPV-positive vulva cancer progression.

The specific objectives were to study:

1. The effect of miR-582-5p modulated vulvar CAFs on HPV-negative vulvar cancer cells.
2. The effect of miR-582-5p modulated vulvar CAFs on HPV-positive (E6E7 expressing) vulvar cancer cells.

3. Materials

Cell culture

Name	Purpose	Catalog#	Supplier
Trypsin-EDTA	Detaching cells from the culture surface	11590626	Thermofisher Scientific
Dulbecco's Modified Eagle Medium High Glucose	Basal growth medium	D6429	Merck
Dimethyl Sulfoxide (DMSO)	Reagent used in cell freezing/preservation	D1435	Merck
Gibco™ DMEM, high glucose, HEPES, no phenol red	Basal growth medium	21063029	Gibco
Sodium Pyruvate (100 mM)	Cell growth media supplement	11360070	Gibco
Phosphate Buffered Saline (PBS)	Cell washing solution	11510546	Thermofisher Scientific
New-Born Calf Serum (NBCS)	Cell growth media supplement	26010074	
Dulbecco's Modified Eagle's Medium/ Nutrient Mixture F-12 Ham	Basal growth medium	D8437	Merck
Bovine serume albumin (BSA)	Cell growth media supplement	41400-045	Merck
Epidermal Growth Factor (EGF) (5ug/ml)	Cell growth media supplement	E4269-1mg	Merck
Insulin-ferritin transferrin (100X)	Cell growth media supplement	41400-045	Gibco
Ascorbic acid (50ug/ml)	Cell growth media supplement	A7631	Sigma- Aldrich
Hydrocortisone (0,4ug/ml)	Cell growth media supplement	H0888	Sigma- Aldrich

L-glutamine (200nM)	Cell growth media supplement	25030-061	Gibco
Collagen Type 1, Rat tail	Preparing matrix	08-115	Merckmillipore
Reconstitution buffer (RB) (2.2 g $NaHCO_3$, 0.6 g NaOH, and 4.766 g 4-(2-hydroxyethyl)-1-piperazineethanesulfonic acid in 100 mL dH_2O)	Neutralizing pH.		
Crystal Violet	Staining fixated cells	B21932.22	Thermo fisher
Formalin solution, neutral buffered, 10%	Fixing 3D organotypics	HT501128	Merckmillipore

Cell culture surfaces

Name	Catalog #	Supplier
NunclonTMDelta 96 well plate	167008	ThermoFisher Scientific
TC-Plate 24 well Standard, F	83.3922.500	Sarstedt
TC-Plate 6 well, Standard, F	83.3920	Sarstedt
TC Flask T25, Standard, Ventilation Cap	83.3910.002	Sarstedt
TC Flask T75, Standard, Ventilation Cap	83.3911.002	Sarstedt
TC Flask T125, Standard, Ventilation Cap	83.3912.002	Sarstedt
Cryovials	5000-0020	Thermofisher Scientific
Incucyte® Imagelock 96-well Plate	BA-04857	Sartorious

Cell counting

Name	Purpose	Catalog#	Supplier
Trypan blue	Reagent for cell viability status	23850	Merck
Dual-Chamber Cell counting slides	Cell counting	1450011	Bio-rad
TC20 (TM) Automated Cell Counter	Cell counting	508BR08712	Bio-rad

Measuring proliferation

Name	Catalog#	Supplier
Resazurin sodium salt	62758-13-8	Merck
Varioskan™ LUX multimode microplate reader	VL0000D0	Thermo fisher

Cell lysate for western blotting

Name	Catalog#	Supplier
RIPA Lysis and Extraction Buffer	89900	Thermofisher
Halt™ Protease and Phosphatase Inhibitor Cocktail (100X)	78446	Thermofisher

Gel electrophoresis and western blotting

SDS-PAGE running gel		
Name	Catalog #	Supplier
SurePAGE™, Bis-Tris, 10x8, 4-12%, 12 wells - 10 PK/BOX	M00653	Genscript

Reagents and buffers		
Name	Catalog #	Supplier
NuPAGE™ LDS Sample Buffer (4X)	NP0007	Fisher scientific
NuPAGE® Sample Reducing Agent	NP0009	ThermoFisher Scientific
1X Tris-MOPS-SDS Running Buffer	M00138	Genscript
20x NuPAGE® Transfer Buffer	10564613	Fisher scientific
4X NuPAGE®LDS Sample Buffer	11549166	Fisher scientific
NuPAGE® Sample Reducing Agent	NP0009	ThermoFisher Scientific
20x NuPAGE® Transfer Buffer	10564613	Fisher scientific
Precision Plus Protein™ Dual Color Standards	1610374	Bio-Rad
Super Signal™ West Femto Maximum Sensitivity Substrate	10095983	ThermoFisher Scientific
Tween 20	P1379	Sigma Aldrich
Methanol 99,8%	322145	Sigma Aldrich
Tris-HCl	1185-53-1	Merck
Trizma Base®	T1503	Merck
Others		
Western Blotting filter paper,7cmx8.4cm	84783	Thermofisher
Pierce™ BCA Protein Assay Kit	23225	Thermofisher
Life Science products Cytiva HYBOND-C EXTRA, 20CMX3M	10564755	Fisher scientific
Instruments		
Syngene G:BOX Chemi XX6	733-2351	Thermo Fisher Scientific

Antibodies used for western blotting

Name	Catalog#	Supplier
β-Actin Antibody Dilution: 1:3000	4967	Cell Signaling Technology
EGF Receptor(EGFR1) Mouse mAb Dilution: 1:1000	2256	Cell Signaling Technology
YAP (D8H1X) XP Rabbit mAb Dilution: 1:1000	14074	Cell Signaling Technology
Anti-Oct-3/4 Antibody (C-10) Dilution: 1:500	Sc-5279	Santa Cruz Biotechnology
Anti-rabbit lgG, HRP-linked Antibody	7074	Cell Signaling Technology
Anti-mouse lgG, HRP-linked Antibody	7076	Cell Signaling Technology

Cell lab instruments

Name	Catalog #	Supplier
Swinging bucket centrifuge	0013235	Eppendorf AG
Incubator	305521-2163	Thermo electron corporation
The Sartorius IncuCyte S3 Live-Cell Analysis System	4647	Sartorious

4. Methods

4.1 Cell lab methods

4.1.1 Cell lines

A previously established epithelial vulvar cancer cell line, UMSCV4 was purchased from Thomas Carey at the University of Michigan (UM-SCV-4 (RRID:CVCL_5976)). To understand the role of E6 and E7 HPV viral oncogenes, E6 and E7 were transfected in UMSCV4 and these cells will be called UMSCV4 E6E7 henceforth. Primary vulvar cancer-associated fibroblasts (VCAFs) were isolated previously in the laboratory. To study the effect of miR-582-5p in VCAFs, VCAF7 were transfected with inhibitors of miRNA-582-5p (VCAF7 I-582) and mimics of miRNA-582-5p (VCAF7 M-582)

4.1.2 Cell thawing, culturing, and counting

The cells used were revived from liquid nitrogen tank. Thawing of the cells was done in 37^{o}C water bath, just long enough for the frozen cell suspension to become molten. Then it was added dropwise with a pipette to a 15ml conical tube with 8 ml of cold growth medium (DMEM with 10% NBCS and 2% L-glutamine (200nM)). This cell suspension was carefully mixed by pipetting up and down before centrifuging for 5 minutes at 1300 rpm. After centrifugation, the supernatant was removed and the pellet was resuspended and then transferred in cell culturing flasks (found in the materials) with growth medium containing 50% DMEM and 50% FAD (Dulbecco's Modified Eagle's Medium/ Nutrient Mixture F-12 Ham with 10% NBCS, 2% L-glutamine (200nM), 0,2% EGF (5ug/ml), 0,08% Hydrocortisone (0,4ug/ml), 0,1% Ascorbic acid (50ug/ml) and 0,05% insulin-ferritin transferrin (100X)

All the used cell lines were cultivated using the same growth medium, FAD/DMEM. The cells were split when they reached 90-95% confluency. For this, the old medium

was removed, and the cells were washed with PBS twice. Then they were detached using 0.05% trypsin-EDTA (volume varying with the size of the culturing flask and time depending upon the cell line). When 90% of the cells were detached the activity of the trypsin was neutralized using an equal volume of cold serum-containing DMEM. Then the cell suspension was spun down in a centrifuge and the supernatant was removed and the cells were resuspended and seeded in a new flask with new FAD/DMEM.

To count cells the TC20 (TM) Automated Cell Counter was used. To do this 10 µl of cell suspension was mixed with 10 µl of trypan blue. 10 µl of this mixture was added to the dual-chamber cell counting slides and put into the automated cell counter.

4.1.3 Conditioned medium

CM was collected from cultured VCAF, VCAF I-582 and VCAF M-582 to study the effect of various secreted growth factors, chemokines, cytokines and extracellular vesicles on the epithelial cancer cells; UMSCV4 WT and UMSCV4 E6E7. To prepare the conditioned medium, 20,000 cells per cm^2 were seeded in flasks and allowed to attach and grow for twenty-four hours in regular growth medium for the respective cells. After 24 hours the regular medium was removed, the cells were washed twice with PBS to remove serum, and serum-free medium (Gibco™ DMEM, high glucose, HEPES, no phenol red with 0,1% NBCS, 1% Sodium pyruvate(100nM) and 1,34% BSA) (this is mixture is referred to as serum-free DMEM onwards) was added to the cells. These were allowed to grow for another twenty-four hours in the incubator before the medium was collected, centrifuged at 3000 rpm and the supernatant collected was called conditioned medium (CM). Due to the instability of the various growth factors present in the CM, utmost care was taken to use the CM in the functional assays within 30m of harvesting.

4.1.4 Proliferation assay

The proliferation assay was done using cell lab methods described earlier; both UMSCV4 cell lines were seeded in separate Nunclon^{TM}Delta 96 well plates, 2500 cells per well in a total of five plates for each UMSCV4 cell line, one for each day of absorbance measurement. These were allowed to attach overnight in the FAD/DMEM medium. Then, to look at the effect the various CMs had on the ability of the UMSCV4 cell lines to proliferate, the FAD/DMEM medium was removed, and the cells were washed with PBS before the CMs were added.

The cells were left in CM. For the next five days, each day one plate had resazurin added to the wells and was incubated for four hours, and then had fluorescence measured with 560 nm excitation and 590 nm as the emission wavelength, this was done with the Varioskan™ LUX multimode microplate reader from Thermo Fisher. After the plate had been measured it was disposed of.

As for data analysis, to normalize and translate the absorbance measured into relative growth, a serum-free control was added to each run to normalize the data and served as a baseline for growth. To normalize the data the measured absorbance was divided by the day 1 measurement of the serum-free control. Then to make the data become relative growth each day of the various conditions was divided by the normalized day 1 of each respective condition, this then became the relative growth in which every increment of increase of one meant that the population of alive cells had doubled.

4.1.5 Colony formation assay

Like the proliferation assay, this was also done in the cell lab; the cells to be assessed were seeded in 6 well plates (TC-Plate 6 well, Standard, F), 100 cells per well. These were allowed to attach overnight in the FAD/DMEM medium. Then the medium was switched out with CM to look at the effect the CM had on the cancer cell's ability to form and expand colonies. After adding CM, they were left to grow for 15 days. The wells were first fixated using PFA 4% dH2O solution and then cleaned with PBS followed by distilled water. Then the colonies in the wells were stained using Crystal

violet for 10 minutes. The excess crystal violet was removed, and the wells were rewashed to remove unbound dye.

The data from this assay, the stained colonies were simply counted, the data plotted for appropriate graphical representation and analyzed.

4.1.6 3D organotypic co-culture assay

To evaluate the cancer cells' ability to invade into the underlying collagen matrix, 3D organotypics (OTs) were engineered. Briefly, 1ml of biomatrix was made up of the following: 0,7 ml of collagen type I, rat tail, 100 µl of DMEM, 100 µl of RB, and 100 µl of NBCS with 0.25 million fibroblasts (VCAF, VCAF I-582 and VCAF M-582). From this, 700ul of biomatrix was added to each well of a 24 well plate(TC-Plate 24 well Standard, F) and allowed to polymerize in the incubator at 37^{o}C for one hour. After polymerization, 1ml of FAD was added to each well and the plate was incubated overnight. The next day the matrix contracted and detached itself from the side of the wells. After this, FAD was removed and UMSCV4 WT and E6E7 cells resuspended in 1ml of FAD/DMEM was added in the respective wells and incubated further for one day. The next day, the epithelial cells should have attached to the top of the matrix. The solid matrix was then carefully lifted and transferred to the top of an elevated metal grid in a 6-well plate (TC-Plate 6 well, Standard, F) with 2 ml of DMEM/FAD without serum at the bottom. The medium should only touch the bottom of the matrix. This tissue lifting creates an air-liquid interface meant to mimic in-vivo settings of epithelial cell differentiation. The organotypics were then allowed to grow for 11 days with the growth medium changed every 3-4 days.

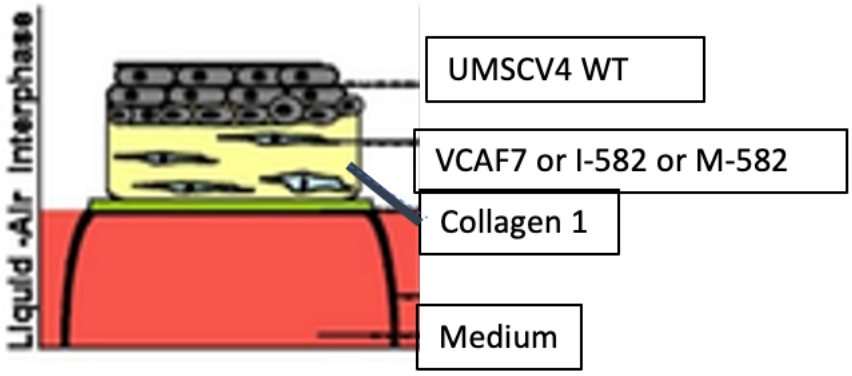

Figure 4. Illustration of the composition of the 3D OT (yellow is the connective tissue equivalent composed of collagen type I and fibroblasts, grey are the cancer cells seeded on top of the collagen matrix and left for a few days submerged to grow then lifted on a metal grid (green structure) at the liquid-air interphase for stratification.

After the organotypic/tissue had grown for 11 days, the tissue was fixed in formalin solution, (neutral buffered, 10%) paraffin-embedded and was then cut to prepare tissue slides which were then investigated and measured for epithelial invasion into the VCAF matrix. For assessing the results of the invasion assay the slides were stained with hematoxylin and eosin (HE) and imaged on a brightfield microscope.

4.1.7 Migration assay

To investigate migratory capabilities, migration assay was performed. First, the Incucyte® Imagelock 96-well Plates (with sensors allowing for pictures to be taken in the same area in the different wells at specific times) were seeded with 15,000 UMSCV4 cells in DMEM/FAD and then put in the incubator to incubate overnight. The next day the cells had attached, and the medium was removed and replaced with various CM made with methods described in the conditioned medium section; the plate was then put back in the incubator for 24 hours. Twenty-four hours later, the plate was collected, and with the Incucyte® Cell Migration Kit. The wound was prepared by creating a scratch in the middle of each well. Then the plates were incubated in the Sartorius IncuCyte S3 Live-Cell Analysis System, which was programmed to capture a picture every hour at specific sites using the sensors in the plates.

After 48 hours, the pictures were collected, and using in-built software, the initial wound size and the gradual decrease in wound size was measured. For data analysis, the hourly software-measured wound width was plotted on a graph.

4.1.8 Cell lysates

To prepare cell lysates for western blotting, the cells were cultured in a 6 well plate(TC-Plate 6 well, Standard, F), where 200,000 cells were seeded per well. After the cells had adhered to the surface, they were exposed to various CM for 48 hours. Then, they were lysed using a cell scraper and 300 µl of RIPA lysis buffer containing Halt™ Protease and Phosphatase Inhibitor Cocktail 1x in each well. The buffer containing cell lysate was collected and centrifuged at 13000 rpm at 4^{o}C to remove cell debris. The supernatant was transferred to fresh tubes and stored at -80^{o} C until further use.

4.2 Western blotting

4.2.1 Protein estimation

To load an equal amount of protein for the western blot, the amount of protein in each cell lysate had to be determined. To do this, Peirce BCA kit was used. First, a standard curve was estimated using serial dilutions of bovine serum albumin (BSA). A serial dilution was made of the BSA containing 7 different dilutions. Then an equal amount (10 µl) of all the unknown protein lysates, as well as the standards, were loaded onto a 96 well plate(Nunclon™Delta 96 well plate). In each well, 200 µl of working reagent (which is 50 parts of BCA reagent A and 1 part of BCA reagent B) was added. This was then incubated at 37^{o}C for 30 minutes in the dark. Then absorbance was measured at 562 nm, the measurement of the standards was used to plot absorbance per mass as the mass for the standards was known. With these plots, linear regression was used to form a function for how much absorbance equates to

how much protein which was then used to estimate the protein contents of the different lysates.

4.2.2 Western blotting

Western blotting was performed and was performed as follows:

The volume that equated to 10 µg of protein was added (volume varies with protein concentration), then an equal volume was added of 2X loading buffer (LB). LB was made up of NuPAGE™ LDS Sample Buffer (4X) diluted in distilled water(dH_2O) and NuPAGE® Sample Reducing Agent, mixed as follows; for 1ml of LB= 450 microliters NuPAGE™ LDS Sample Buffer (4X), 450 µl of dH_2O and 100 µl of NuPAGE® Sample Reducing Agent. This equal mix of protein solution and 2X LB was heated for 10 minutes at 70^{o}C with shaking and was then loaded onto the pre-casted gels from Nupage 4-12% polyacrylamide gel assembled in the XCEll SureLock mini-cell gel module. 4 µl of Page Ruler™ Plus Prestained Protein Ladder was also loaded. The gel was then ran on 80V for 30 minutes and then 140V for another 30 minutes until the last band of the prestained protein ladder had reached the bottom of the gel.

The proteins in the gel were then transferred to a PVDF transfer membrane. This was done by removing the gel and then forming a transfer sandwich as described by the manufacturer's protocol. The tank was then filled with transfer buffer which is a mixture of 20x NuPAGE® Transfer Buffer diluted to 1X in dH_2O with 10% methanol. This was ran at 30V for two hours on ice. Finally, the transfer sandwich was disassembled, and the transfer membrane was washed with 1X TBST for 15mins to remove excess transfer buffer. 1X TBST was made from 10X TBS stock which was made up of 120g Tris-HCl, 20g Trizma base, 440g NaCl dissolved in 4500ml of dH_2O (adjust the pH to 7,6). This stock was then diluted to 1X with dH_2O and 0.1% Tween 20 was added. The transfer-membrane was now blocked to reduce unspecific binding. This was done by incubating the membrane with 5% BSA diluted in TBST

for 1h at room temperature. After blocking the membrane, it was cut to separate the different sections to incubate it with different primary antibodies depending upon the protein/s of interest. The primary antibodies (can be seen in materials) were diluted according to manufacturer's instruction in the same mixture that the blot was blocked in and then left overnight on slow rocking at 4°C.

Figure 5. Schematic picture of western blot wet transfer sandwich (ref: https://www.sinobiological.com/category/wb-wet-transfer)

The day after, the membranes were washed thrice in 1X TBST, and they were then incubated for 1h at RT in the appropriate secondary antibody in 1:3000 dilution in 5% non-fat dry milk in TBST. They were then washed again thrice in 1X TBST for 10 minutes each time. For signal development Super Signal™ West Femto Maximum Sensitivity Substrate from Thermo Fisher was used following manufacturer's instructions. The blots were incubated in working solution for 1-3 min which is a 1:1 solution of peroxide solution and luminol solution provided in the kit, then they were placed in clear plastic film before being exposed to the imaging system from Syngene; Syngene G:BOX Chemi XX6.

5. Results

Expression of miR-582-5p in vulvar SCC

The role of miR-582-5p in vulvar carcinogenesis was first studied using qPCR to determine relative miRNA expression in vulvar cancer cells and vulvar CAFs. For this, cells were derived from vulvar tissue biopsies from patients treated at Haukeland Universitetssjukehus (HUS). qPCR revealed 'no expression' of miR-582-5p in vulvar cancer cells. Interestingly, qPCR showed higher expression of miR-582-5p in vulvar CAFs as compared to normal fibroblasts isolated from the same patient (Figure 5). When paired, the vulvar CAFs from patient 7 (VCAF7) showed the highest differential expression of miR-582-5p as compared to their normal counterpart fibroblasts (NF7) (Figure 5). This raised interest in deciphering the role of miR-582-5p in the TME in vulvar SCC.

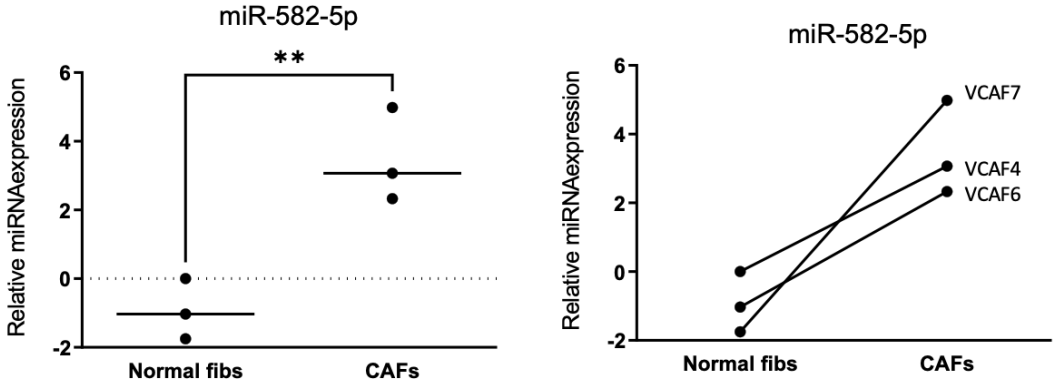

*Figure 6. Relative miRNA expression of miR-582-5p from vulvar CAFs and normal vulvar fibroblasts derived from tissue biopsies collected at Haukeland Universitetssjukehus. Non-parametric Student's unpaired t-test was used to determine significance.**p=0.0095.*

Modulation of miR-582-5p expression in VCAFS by mimics and inhibitors

To look at how miR-582-5p modulates VCAF7 influence on cancer cells, VCAF7 cells were transfected with mimics and inhibitors of miR-582-5p. Figure 6 shows the relative miR-582-5p expression in VCAF7, VCAF7 M-582 (VCAF7 transfected with mimics of miR-582-5p) and VCAF7 I-582 (VCAF7 transfected with inhibitors of miR-582-5p). The expression of miR-582-5p in the VCAF7 transfected with mimics of miR-582-5p is ~17 fold greater than in wild-type VCAF7. Meanwhile, it was downregulated ~97 folds in the ones transfected with the inhibitors, showing the efficiency of transfection.

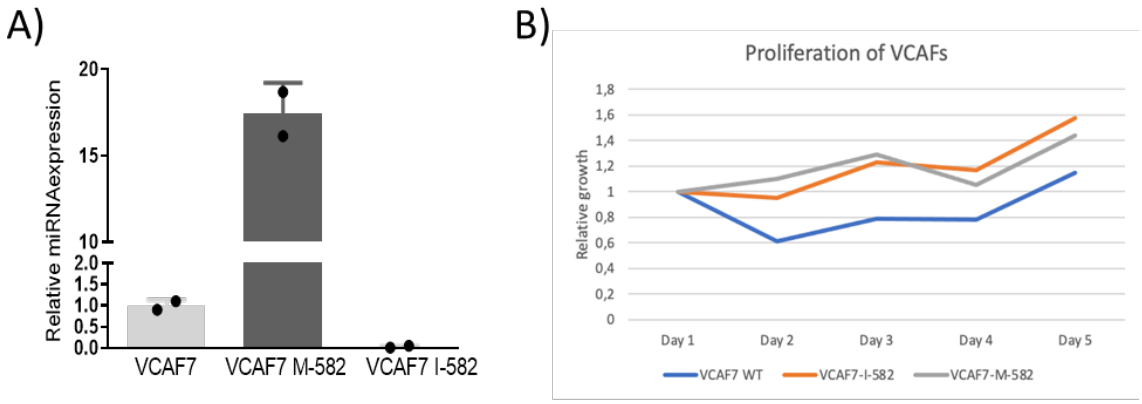

Figure 7. A) Relative miRNA expression of VCAF7 wild type, VCAF-7 transfected with mimics of miR-582-5p (VCAF7 M-582) and VCAF7 transfected with inhibitors of miR-582-5p inhibitors (VCAF7 I-582). qPCR was performed twice with two technical replicates each. B) Graph showing no difference in proliferation in VCAF7 M-582 as compared to VCAF7 I-582.

A proliferation assay was performed on the transfected VCAF7 cells. This was done to show the difference in proliferation, which can affect the cells' secretomes in the CM, as higher proliferation can lead to higher cell density, leading to more concentrated CM. Figure 6 B) shows the proliferation assay results with relative growth plotted per day; the fastest-growing were the VCAF7 I-582 but there was no significant difference when compared to VCAF7 M-582.

E6 and E7 oncogenes increase proliferation, colony formation and migration of HPV-negative UMSCV4 cells

The HPV viral proteins, E6 and E7 are directly responsible for HPV-induced carcinogenesis (Tomaić, 2016). To study the effect of E6 and E7 in VSCC, the HPV-independent cells UMSCV4 (now UMSCV4 WT, also referred to as WT) cell line were transfected with E6 and E7 viral oncogenes, now called UMSCV4 E6E7. To verify that the transfection was successful, western blot was done. As seen in figure 7, the E6 and the E7 genes were both expressed in the transfected cells (UMSCV4 E6E7, also referred to as E6E7). A nonspecific band on the wild type cells is thought to be due to an overflow in loading of the wells of the gel. β-actin was also visualized as a control to verify that equal amounts of proteins were loaded.

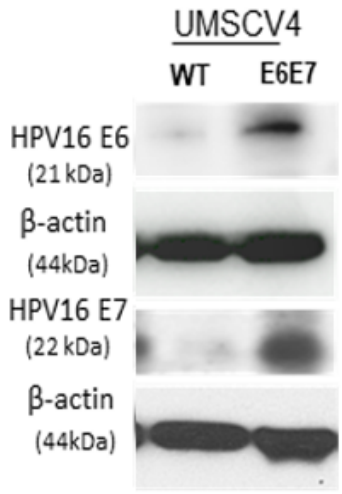

Figure 8. Western blot of UMSCV4 wild type cells and UMSCV4 cells transfected with the E6 and the E7 viral genes

To study the effect of the E6 and E7 viral oncogenes in HPV-negative UMSCV4, colony formation and proliferation assays were performed on both WT and E6E7 (figure 8). The assays were performed with two biological replicates with further three technical replicates for the colony formation and five technical replicates for the

proliferation assay. In the colony formation assay, colonies were generally bigger in the E6E7 transfected cells (figure 8A) whereas in the proliferation assay, there was a clear indication of greater proliferative potential in the cells transfected with E6 and E7 oncogenes (figure 8B).

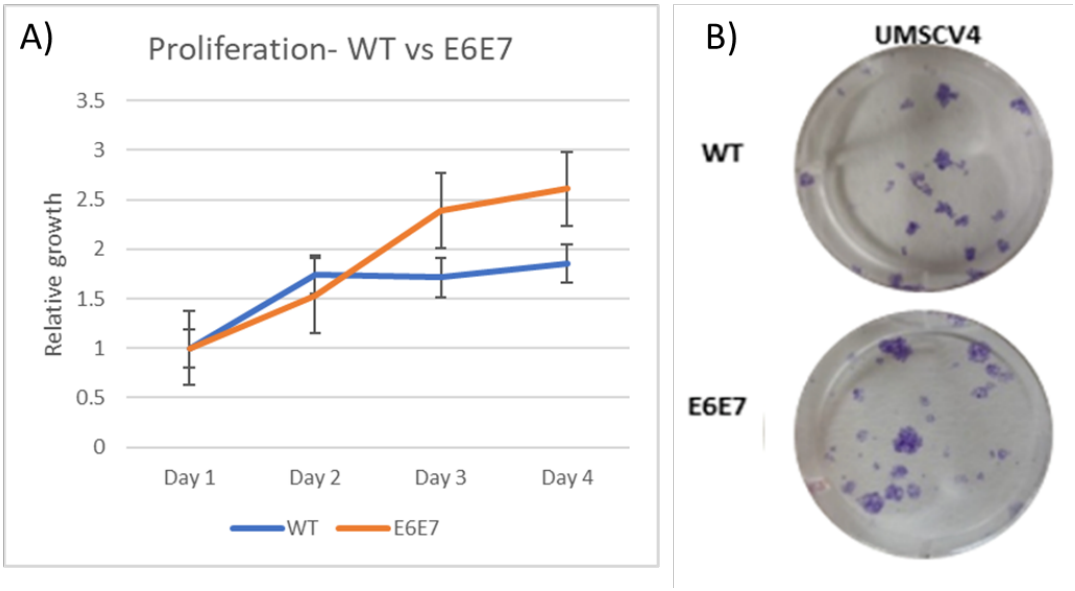

Figure 9.Proliferation and colony formation assay. A) Proliferation assay showing increase in proliferation of E6E7 cells as compared to WT cells. The graph is plotted with mean ± standard error over mean (SEM) of all replicates. B) The results shown here are representative of colony formation assay of WT and E6E7 cancer cells.

The scratch wound assay was done to look at the effect of E6E7 on the migration of transfected cells. The cells were grown in serum-free medium to minimize the effect of the serum in the medium. Here there were five technical replicates but no extra-biological replicates due to unavailability of the imaging system. At t=36 hours, the wound with UMSCV4 E6E7 cells had closed, meanwhile, the UMSCV4 WT wound was still open (figure 9A). The graph of measured wound width in µm every two hours until both wounds had closed is shown in figure 9B. The graph shows that across all replicates, plotted on average, the UMSCV4 E6E7 closed the wound at 36 hours; meanwhile, in the UMSCV4 WT, the wound closed at t=44. This suggests that E6E7 increases migratory potential of UMSCV4 cells in a 2D scratch wound assay.

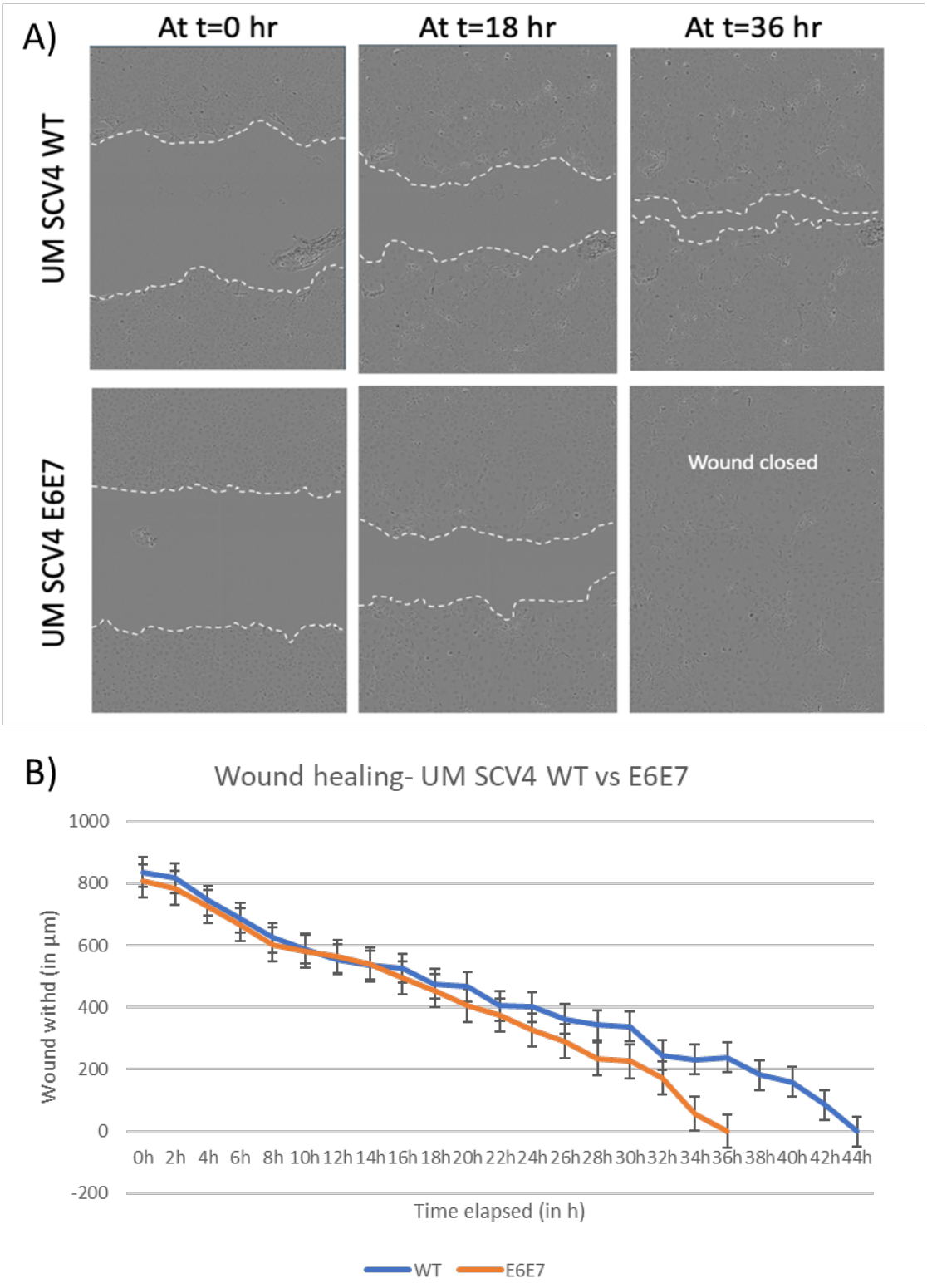

Figure 10. A) Phase-contrast images of scratch wound assay performed on UMSCV4 WT and UMSCV4 E6E7 cells showing wound closing at different time points. These images were taken over a period of two days in the IncuCyte system. B) The graph shows wound width measured in µm over time of UMSCV4 WT and UMSCV4 E6E7 cells in the scratch wound assay. The graph is plotted with the mean ± SEM of all replicates.

Effect of miR-582-5p modulated VCAFs on VSCC cells

To investigate the effect that miR-582-5p modulated VCAF7 has on UMSCV4 WT and E6E7 cell lines, various functional assays with CM from the different VCAF7 cell lines were performed.

Proliferation assay

First proliferation assays were performed with CM from VCAF7, VCAF7-I-582, and VCAF7-M-582, and the data is presented in Figures 10 to 13. Each proliferation experiment was performed with two biological replicates along with five technical replicates each. The relative growth was calculated as described in the methods section 4.1.4. There is also a WT CM and an E6 CM control which is CM made from the UMSCV4 cell line that is being tested and thus represents the effect of solely autocrine signaling.

In the proliferation assay done to assess growth of UMSCV4 WT cells with CM from monoculture, the normalized growth was greatest in the WT + WT CM with a 3.5-fold growth at day 5, followed by the WT + VCAF7 CM with threefold growth (Figure 10). This suggests that the CM from VCAF7 did not increase proliferation of WT cells in culture. Interestingly, both VCAF7 I-582 CM and VCA7 M-582 CM did not influence the proliferation of WT cells. In fact, the WT cells proliferated less in both these CMs.

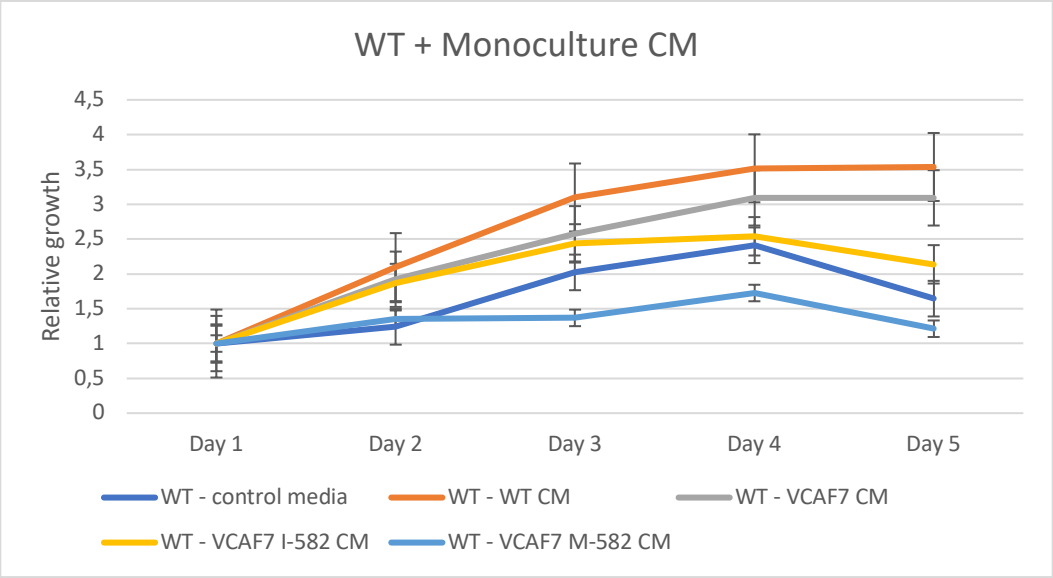

Figure 110. Proliferation of UMSCV4 WT cells conditioned by various monoculture CMs. Relative growth was plotted on the y-axis over five days using mean ± SEM of all replicates.

Similarly, for the proliferation of UMSCV4 E6E7 cells in the CM from monocultures, the normalized growth was the greatest in the E6E7 CM with an almost 2.5-fold growth at day 5 (Figure 11). VCAF7 I-582 CM also increased the proliferation of E6E7 cells much more as compared to VCAF7 M-582 CM but comparable to VCAF7 CM.

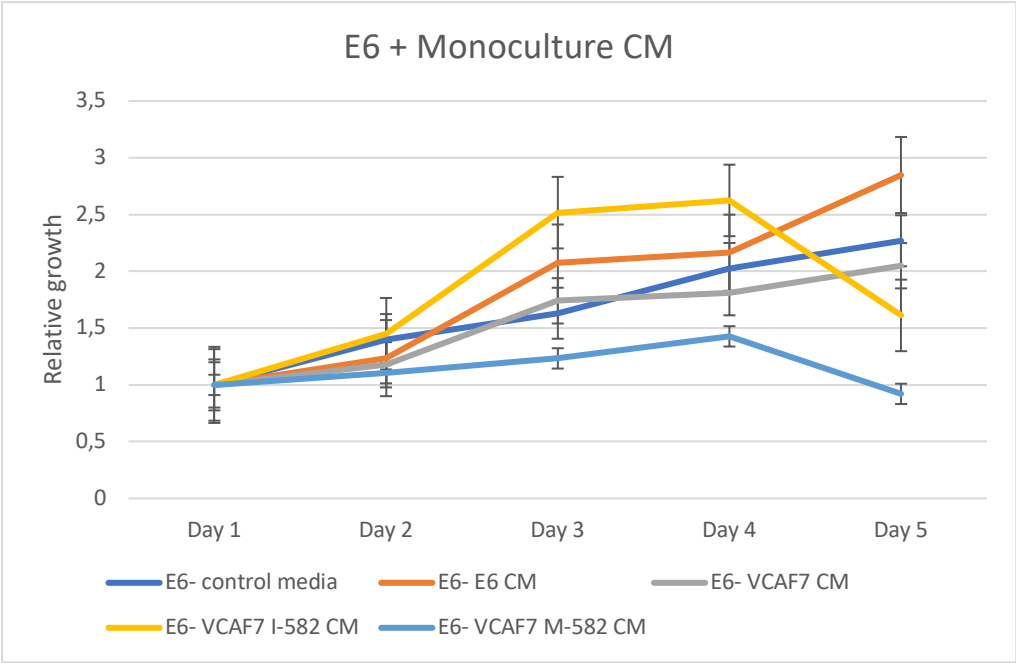

Figure 121. Proliferation of UMSCV4 E6E7 cells conditioned by various monoculture CMs with serum-free growth medium as control. Relative growth is plotted on the y-axis over five days using mean ± SEM of all replicates .

For the proliferation of WT cells in co-culture CM, the normalized growth was greatest in the WT+VCA7 co-culture CM with an almost fourfold growth at day 5 (Figure 12). Both VCAF7 I-582 and VCAF7 M-582 increased proliferation of WT cells as compared to the WT controls but not as much as WT+VCAF7 co-culture CM.

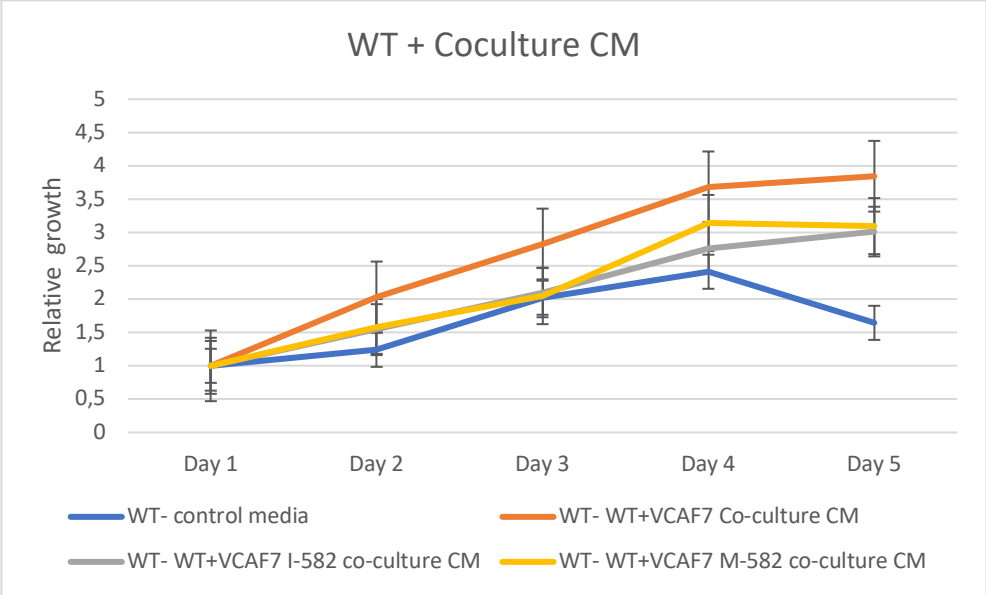

Figure 132. Proliferation assay of UMSCV4 WT cells conditioned by various co-culture CMs with serum-free growth medium as control. Relative growth is plotted on the y-axis over five days using mean ± SEM of all replicates.

In the proliferation assay of E6E7 cells grown in CM from co-cultures, the relative standardized growth was greatest in the E6E7+VCA7 CM with a threefold growth observed at day 5. Surprisingly, E6E7+VCAF7 M-582 CM had higher proliferation rate as compared to E6E7+VCAF7 I-582 CM (figure 13).

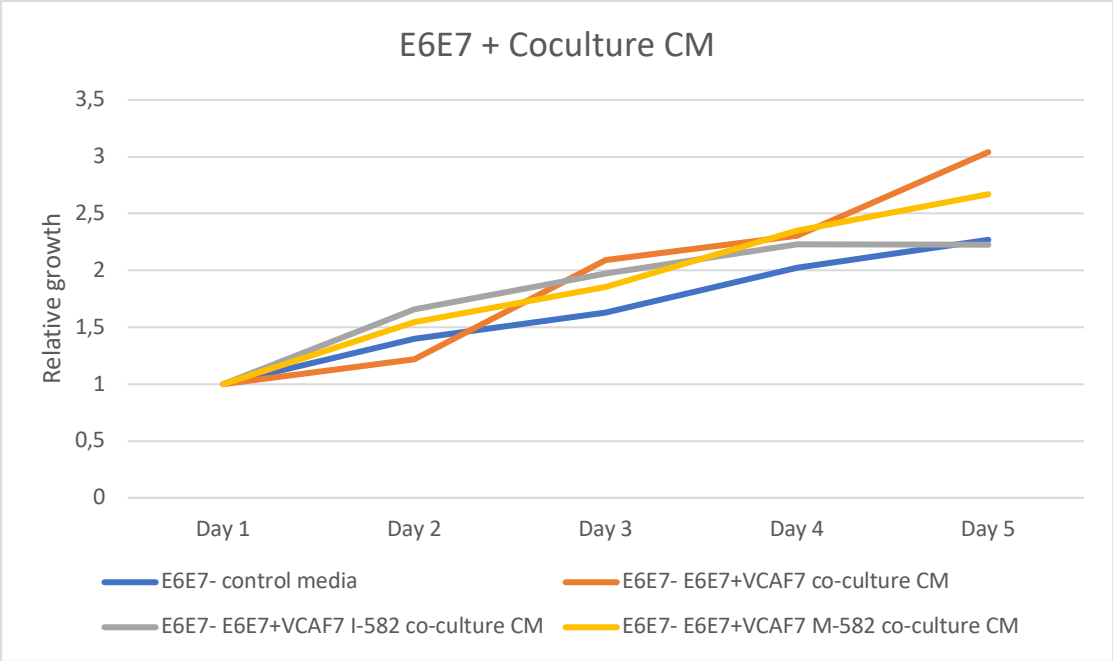

Figure 13. Proliferation assay with UMSCV4 E6E7 cells conditioned by various co-culture CMs with serum-less growth medium control(E6 control) and UMSCV4 E6E7 monoculture CM control(E6 w/E6 CM). Relative growth is plotted on the y-axis over 5 days.

Overall, in the proliferation assay, the VCAF7 co-culture CMs proliferated more than the monocultures for both UMSCV4 WT and the UMSCV4 E6E7. When comparing the CMs effect in UMSCV4 WT versus the UMSCV4 E6E7, the CMs seem to increase proliferation of the UMSCV4 WT cell line.

Colony formation assay

The second functional assay performed was colony formation. Here, as a control, UMSCV4 cells were grown in both serum-free medium and CM from WT and E6E7. There were no colonies formed in any VCAF7 CM monocultures and the serum-free controls. For the co-cultured CM, the assay was done with two biological replicates and two technical replicates each. However, for the VCAF-I-582, there was only a single biological replicate with two technical replicates due to technical errors.

UMSCV4 WT cells formed only 7.5 ± 2.12 colonies when cultured in WT CM , 13.5 ± 0.7 in WT+VCAF7 CM, 3 ± 1.41 in WT+VCAF7 I-582 CM and 16 ± 1.4 in WT+VCAF7 M-582 CM (Figure 14). Moreover, the size of colonies formed in WT+VCAF7 M-582 was biggest among all.

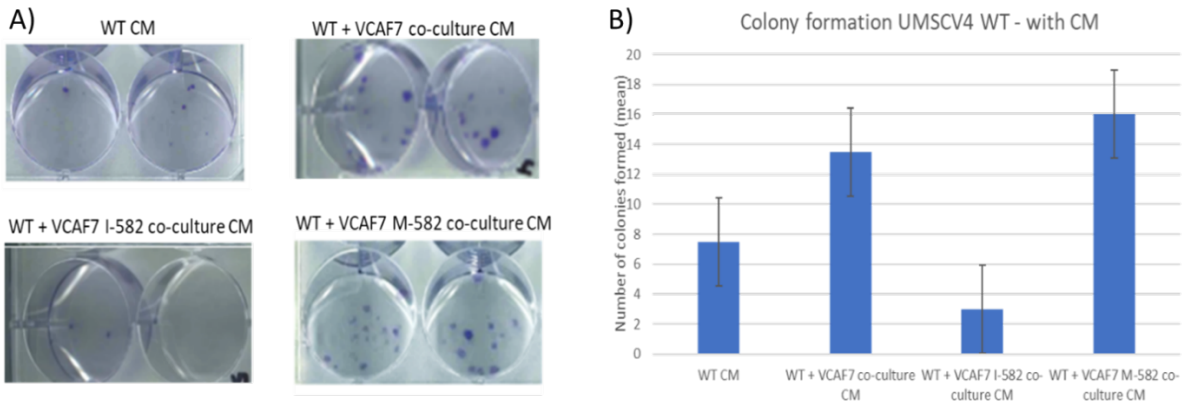

Figure 14. A) Colony formation capacity of UMSCV4 WT when grown in different CM from co-cultured settings. B) Graphical representation of number of colonies formed in each condition.

UMSCV4 E6E7 cells formed 8.5 ± 0.7 colonies when cultured in E6E7 CM , 13.5 ± 2.12 in E6E7+VCAF7 CM, 7 ± 1.41 in E6E7+VCAF7 I-582 CM and 20 ± 5.65 in E6E7+VCAF7 M-582 CM. In addition, the size of colonies formed was biggest in E6E7+VCAF7 M-582 (figure 15).

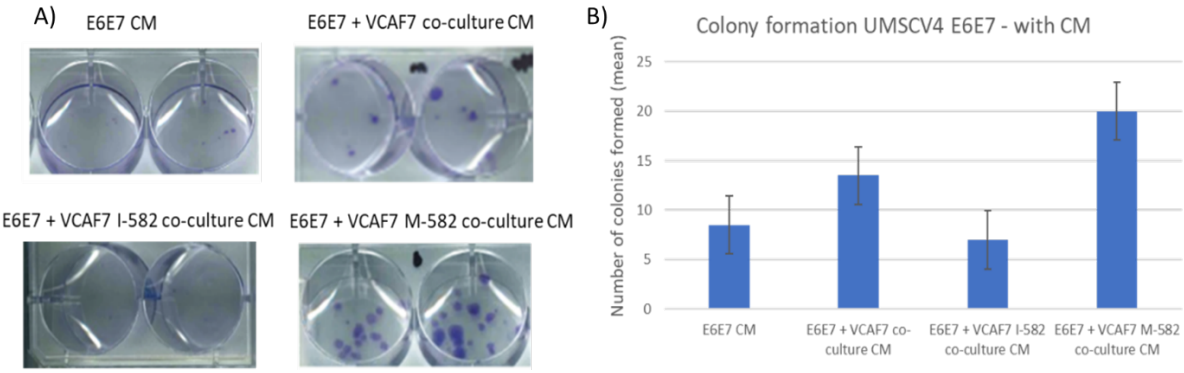

Figure 145. A) Colony formation capacity of UMSCV4 E6E7 when grown in different co-cultured CM. B) Graphical representation of number of colonies formed in each condition.

Migration assay

Scratch wound assay was performed to investigate the effect of miR-582-5p modulated VCAFs on migratory capacity of vulvar cancer cells. Here as a control, WT cells were grown in serum-free medium. Phase-contrast images showed that the wound closed fastest in VCAF7 M-582 CM at t=10h followed by VCAF7 CM (t=14h)and VCAF7 I-582 CM (t=18h) (figure 16). The WT cells grown in serum-free medium closed the wound at 44h (figure 16). The VCAF7 M-582 CM closed the wound 4 and 8 hours faster than the VCAF7 CM and VCAF7 I-582 CM conditioned cells, respectively.

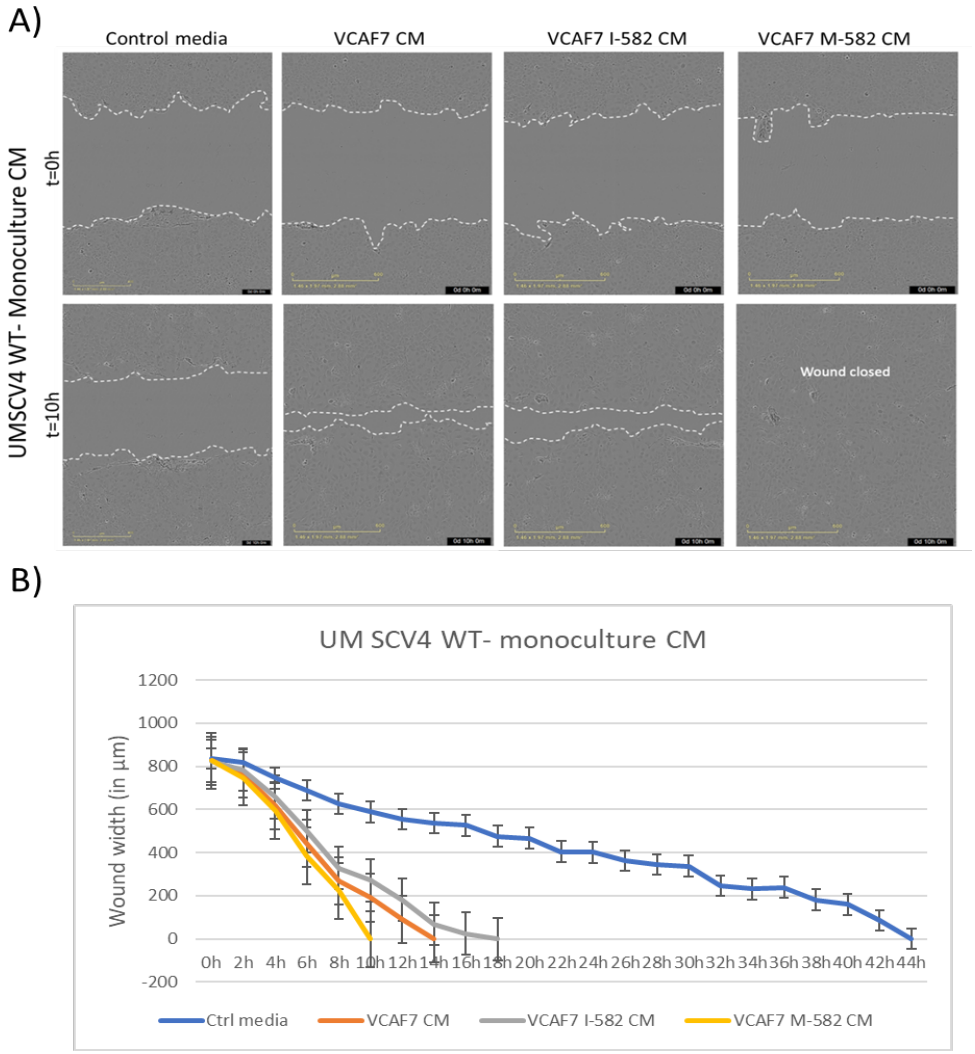

Figure 16.A) Phase contrast images of scratch wound assay performed on UMSCV4 WT with different CM. These images were taken over a period of two days in the IncuCyte system. The white dotted line shows the cell borders of the wound. B) Graphical representation of closure of wound width of WT cells grown

with different CM calculated by IncuCyte software. The data is plotted with mean ± SEM values of all technical replicates.

Similar scratch wound assay was performed for E6E7 cells with CM from different conditions. As a control E6E7 cells were grown in serum-free medium. Phase-contrast images showed that the wound closed the fastest again in VCAF7 M-582 CM at t=10h followed by VCAF7 CM (t=14h)and VCAF7 I-582 CM (t=18h) (figure 17). The WT cells grown in serum-free medium closed the wound at 36h (figure 17). Similar to WT cells, it is clear that the VCAF7 M-582 CM closed the wound 4 and 8 hours faster than the VCAF7 CM and VCAF7 I-582 CM conditioned cells, respectively in E6E7 cells as well.

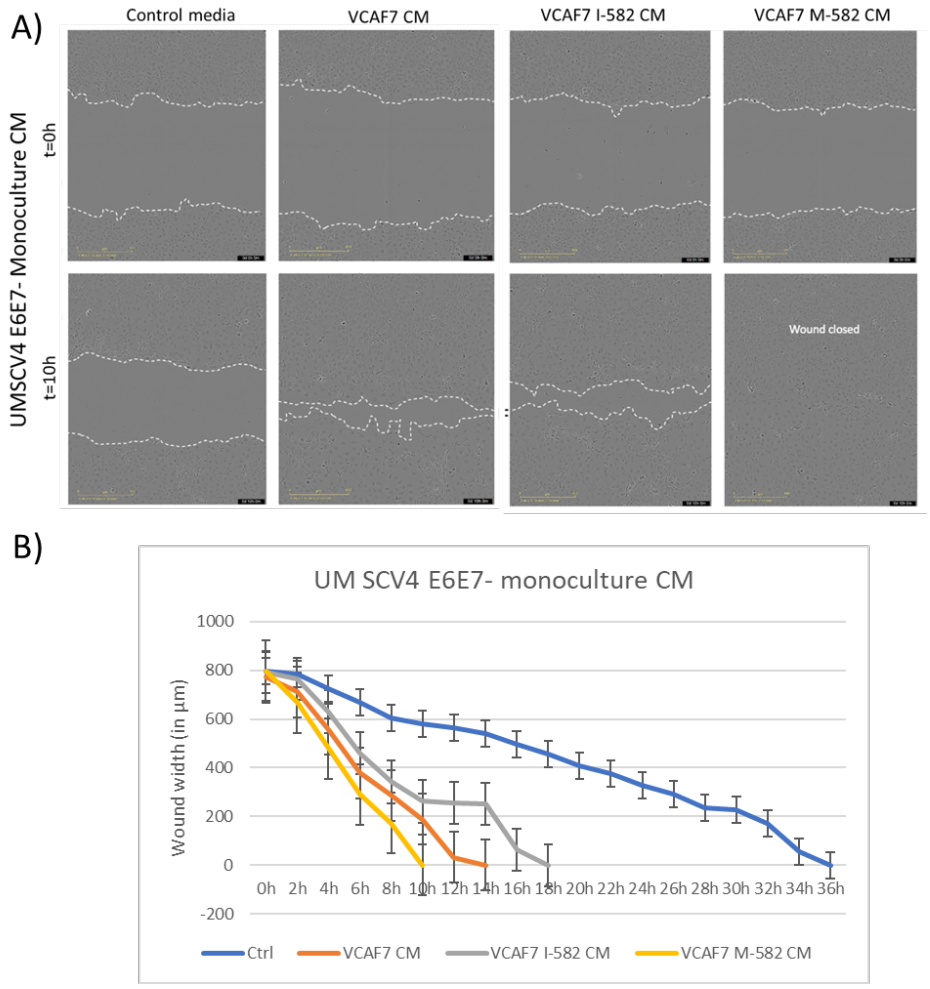

Figure 17. A) Phase contrast images of scratch wound assay performed on UMSCV4 E6E7 with different CM. These images were taken over a period of two days on the IncuCyte system. The white dotted line shows the cell borders of the wound. B) Graphical representation of closure of wound width of E6E7 cells grown with different CM calculated by IncuCyte software. The data is plotted with mean ± SEM values of all technical replicates.

Surprisingly, when WT cells were grown in CM from co-cultures, the wound closed slower. Nonetheless, among various conditions the wound closed fastest in WT+VCAF7 M-582 CM at t=14h followed by WT+VCAF7 CM (t=16h) and WT+VCAF7 I-582 CM (t=20h) (figure 18). The WT cells grown in serum-free medium closed the wound at 36h (figure 18).

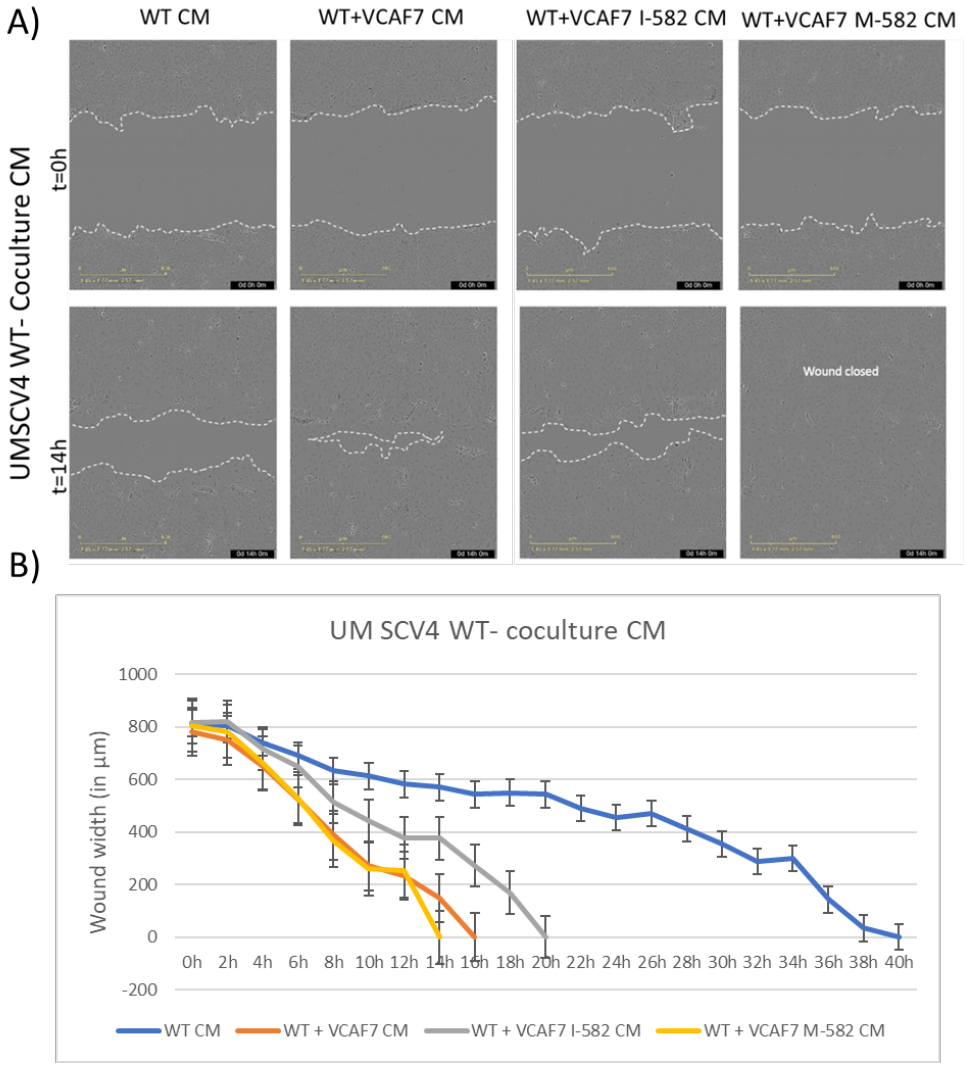

Figure 18. A) Phase-contrast images of scratch wound assay performed on UMSCV4 WT with different CM from cocultures. These images were taken over a period of two days in the IncuCyte system. The white dotted line shows the cell borders of the wound. B) Graphical representation of closure of wound width of WT cells grown with different CM calculated by the IncuCyte software. The data is plotted with mean ± SEM values of all technical replicates.

Among various conditions the wound closed fastest in E6E7+VCAF7 M-582 CM at t=14h followed by E6E7+VCAF7 CM (t=18h) and E6E7+VCAF7 I-582 CM (t=20h) (figure 19). The E6E7 cells grown in serum-free medium closed the wound at 34h (figure 19).

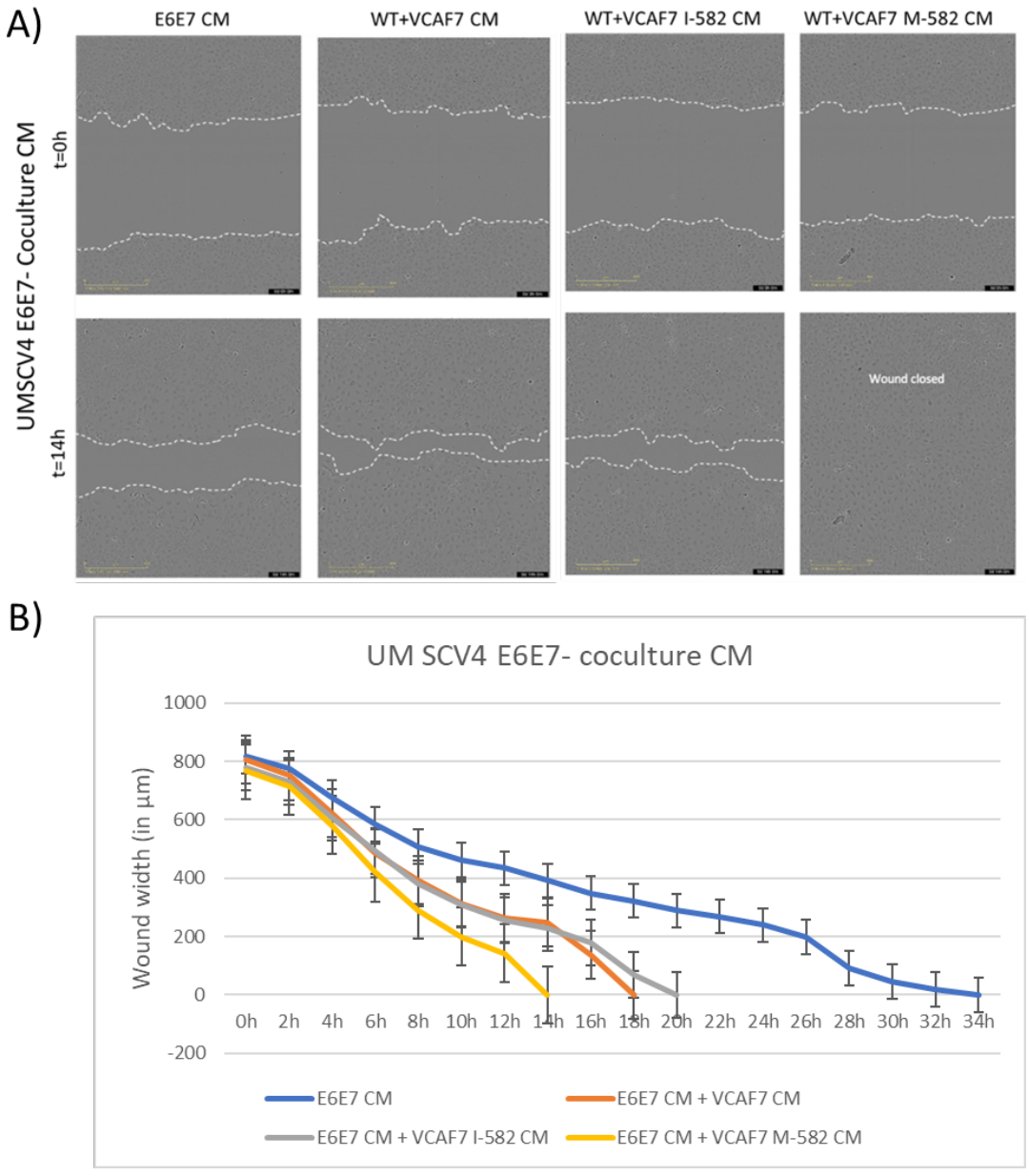

Figure 19. A) Phase contrast images of scratch wound assay performed on UMSCV4 E6E7 with different CM from cocultures. These images were taken over a period of two days on the IncuCyte system. The white dotted line shows the cell borders of the wound. B) .Graphical representation of closure of wound width of E6E7 cells grown with different CM calculated by IncuCyte software. The data is plotted with mean ± SEM values of all technical replicates.

Of all the conditions, CM from both the VCAF7 M-582 monocultures and cocultures closed the wound fastest in WT and E6E7 cells.

Invasion assays

To assess the invading capabilities of WT and E6E7 cells influenced by miR-582-5p modulated VCAF7s, 3D organotypic coculture models were used. The underlying collagen matrix contained different VCAFs (figure 20). The WT cells grown on VCAF7 I-582 invaded more as compared to both VCAF7 M-582 and VCAF7 I-582 (figure 20 A). However, the WT cells differentiated comparably when grown on VCAF7 M-582 and VCAF7 but not when grown on VCAF7 I-582. Similarly, E6E7 cells invaded more into the matrix populated with VCAF7 I-582 in comparison to VCAF7 M-582. However, the E6E7 cells differentiated the most when grown on VCAF7 M-582 populated collagen matrix (figure 20 B).

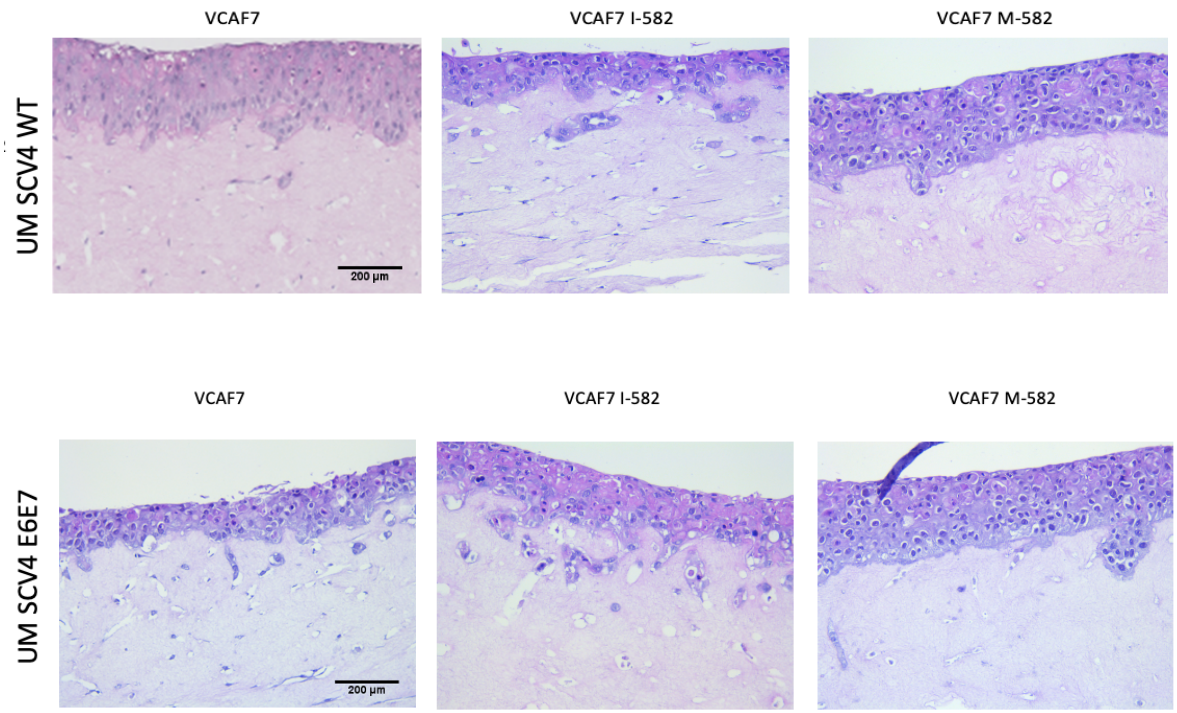

Figure 20. Hematoxylin and Eosin (HE) stained slides of 3D OTs. Histology of 3D OTs grown on different VCAFs show formation of stratified epithelial A) UM SCV4 WT and B) UM SCV4 E6E7 cells on the underlying collagen matrix. Scale bar = 200 µm.

Changes in protein expression (Western blot)

Western blotting was performed to study protein expression of EGFR, YAP and Oct 3/4 (figure 21 and 22). For the UMSCV4 WT cells, there was a higher expression of EGFR in the UMSCV4 WT cells conditioned with VCAF7-I-582 CM in both the monoculture and the co-cultures. For both Oct 3/4 and YAP, there was not much difference between any conditions. However, there seems to be a trend of more expression across the board on the monoculture VCAF7 CMs versus the co-cultured VCAF7 CMs (figure 21). The beta-actin serves as a loading control to show that the difference in band size in various proteins of interest is not merely due to differences in the amount of protein loaded.

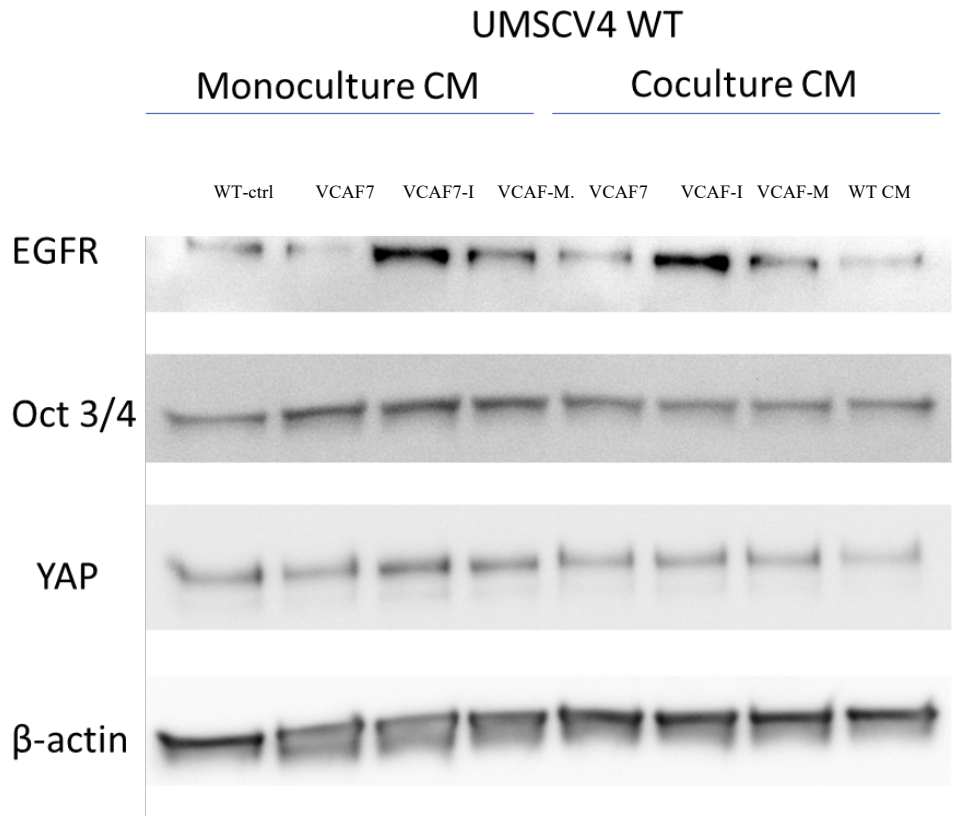

Figure 21. Western blot done on cell lysates of UMSCV4 WT cells conditioned with various VCAF7 CMs from both monocultures and cocultures. From the left, the first well is UMSCV4 WT grown in serum-less medium, and then monoculture VCAF7 CM, monoculture VCAF7-I-582 CM, monoculture VCAF7-M-582 CM, co-culture WT+VCAF7 CM, co-culture WT+VCAF7 I-582 CM, co-culture WT+VCAF7 M-582 CM. The proteins looked at are on the left.

In the western blot performed on the cell lysates from UMSCV4 E6E7 (figure 22), cells conditioned in various VCAF7 CMs have the same loading scheme as the UMSCV4 WT western blot mentioned above. There was a higher expression of EGFR in the UMSCV4 E6E7 cells conditioned with VCAF7 I-582 CM in both the monoculture and the co-culture CM. For both Oct 3/4 and YAP, there was not much difference between any of the conditions. However, there does seem to be a trend of more expression across the board on the monoculture VCAF7 CMs versus the co-cultured VCAF7 CMs.

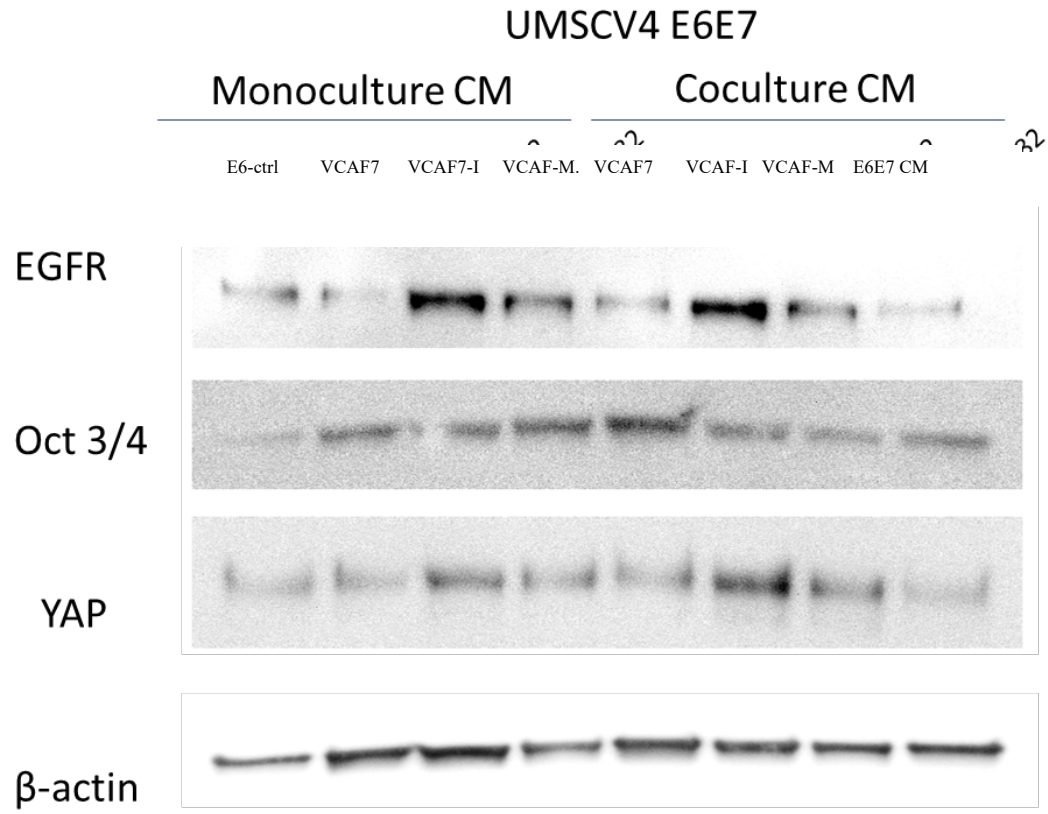

Figure 22. Western blot performed on cell lysates of UMSCV4 E6E7 cells conditioned with various VCAF7 CMs, both monocultures and co-cultures. From the left, the first well is UMSCV4 E6E7 grown in serum-free medium, and then monoculture VCAF7 E6E7 CM, monoculture VCAF7 I-582 CM, monoculture VCAF7 M-582 CM, co-culture E6E7+VCAF7 CM, co-culture E6E7+VCAF7 I-582 CM, co-culture E6E7+VCAF7 M-582 CM. The proteins probed are mentioned on the left.

6. Discussion

Role of E6 and E7 in tumorigenicity

HPV-independent and HPV-dependent VSCC have different pathological pathways of carcinogenesis. Although the mechanism of immortalization and subsequent transformation through E6 and E7 oncogenes is known, the role of cancer-associated fibroblasts (CAFs) and especially of micro-RNAs is still unknown. Previous work done in our group reported twelve different miRNAs with differential expression in oral SCC CAFs as compared to normal fibroblasts (Rajthala et al., 2021). One of the miRNA; miR-582-5p was significantly upregulated in oral CAFs suggesting important repercussion in SCC oncogenesis. However, the role of this miRNA in HPV-independent and HPV-dependent VSCC is unknown. This thesis is an attempt to bridge this knowledge gap.

The first part of thesis deals with studying the role of E6 and E7 oncogenes in a vulva cancer cell line, UMSCV4. Upon viral transformation after introducing two viral genes E6 and E7, the UMSCV4 E6E7 cell line proliferated more in comparison to the non-transfected, UMSCV4 WT cells. Additionally, the E6E7 cells also formed more colonies as demonstrated by the colony formation assay. The scratch wound healing assay demonstrated that E6E7 oncogenes make the cells migrate faster, as reported earlier by Hu et al. (Hu et al., 2015). Although, the wound healing could be a dual effect of cells proliferating and migrating, though, cancer cells generally do not divide in absence of serum in the culture medium.

Role of I-582 and M-582 VCAFs in VSCC proliferation

The first assay performed to examine the effect on VSCCs of miR-582-5p modulation in VCAFs was proliferation assay. The monoculture CM setting was used to study the effect of unidirectional crosstalk between CAFs and cancer cells whereas the coculture CM setting was used to study the bidirectional crosstalk. Overall, it seems

that the co-culture CMs promote proliferation of both WT and E6E7 UMSCV4 cell lines, with highest proliferation seen by VCAF7 CM, followed by the VCAF7 I-582 CM and VCAF7 M-582 CM. Similar observations were made with the monoculture CM, suggesting that modulating miR-582 does not increase proliferation of cancer cells. However, as expected the CM from cocultures increase proliferation of both WT and E6E7 cells indicating the importance of reciprocal signaling and cross-talk to make the stromal VCAFs more cancer-supporting.

Role of I-582 and M-582 VCAFs in effecting vulva cancer cells' ability to form colonies

None of the CM from monocultures could form any colonies at all except the ones grown in UMSCV4 WT and E6E7 CM, wherein only small colonies were formed. These data suggests that the crosstalk between the cancer cells and the VCAFs is important as the VCAF monoculture conditioned cancer cells had no growth of colonies consistently over many biological replicates and the WT and E6E7 CM had little growth. This makes it seem that the co-cultures and the cancer cell-VCAF crosstalk are very important to the cells being able to survive after being seeded with very few cells and the ability to proliferate continuously to from a single cell colony i.e clonogenicity. When comparing different coculture CM, the VCA7 I-582 CM barely formed any colonies as compared to both VCAF7 and VCAF7 M-582 CM. VCAF7-M-582 CM conditioned UMSCV4 WT and E6E7 generally formed more and larger colonies, with the effect being far more noticeable in the UMSCV4 E6E7. This favoring of the UMSCV4 E6E7 cells could be due to the effect of miR-582-5p modulation in VCAFs being more potent on HPV positive UMSCV4, meaning that higher expression of miR-582-5p could be a worse marker in HPV positive tumors, although this is very speculative and needs to be further validated.

When comparing the cancer cell lines VSCCs (UMSCV4 WT and the UMSCV4 E6E7) conditioned with the VCAF7 CM, there is little difference between the two cell lines. However, VCAF7 co-culture CM does increases proliferation of UMSCV4 WT than UMSCV4 E6E7.

Role of I-582 and M-582 VCAFs in effecting vulva cancer cell migration

This assay revealed that the VCAF7 M-582 CM closes the wound the fastest, followed by VCAF7 CM and then the VCAF-I-582 CM of both WT and E6E7 cells. Different to the aforementioned assays is that the monocultures consistently outperformed the co-cultures, which is inverse in the case of the proliferation and colony formation assays. This is very interesting as the proliferative potential has been established to be less in the cancer cells treated with monoculture CM versus the co-culture CM. This means most likely that this increased ability to close wounds in the monoculture CM is due to increased cell motility and that it is the VCAFs that specifically secrete these factors that cause this effect in the cancer cells. This effect is seen across all three VCAF7 CMs but is slightly more in the VCAF7 M-582 CM. When comparing the UMSCV4 WT to the UMSCV4 E6E7 seen in figures 20 to 31 conditioned cells, one sees that they are remarkably similar, indicating that this effect of increased motility due to VCAF secretome is regardless of HPV status.

Role of I-582 and M-582 VCAFs in effecting vulva cancer cell invasion

For the invasion assay, the VCAF7 I-582 populated collagen matrix increased the invasion of overlying cancer cells irrespective of HPV status. This is interesting as the least tumor promoting condition so far seems to be the VCAF7 I-582, but the ability to induce invasion into the underlying stroma, appears to be the highest in the VCAF7-I-582. The fact that it seems to be that miR-582-5p increases proliferation, but its absence increases invasive capabilities are consistent with the fact that miRNAs have many targets and cause complex changes in the cell. Also mentioned in the results is that the UMSCV4 E6E7 cells seem to, across the board be more invasive than the UMSCV4 WT. Whether this observed effect is due to an intrinsic effect of the E6E7 genes that acts merely additively to the influence of miR-582-5p down regulated VCAF7, or if the influence of miR-582-5p downregulated VCAFs is

greater in HPV positive VSCC versus HPV negative VSCC is hard to tell based on the current data.

Differential protein expression to shed light on molecular mechanisms of the induced effects in VSCC.

Lastly, the protein expression of different markers could shed some light on the molecular mechanism behind the differences seen in the various assays. As for the molecular mechanism behind the increase in VCAF7s ability to induce invasiveness through miR-582-5p inhibition, in the western blot, there is an increase in both VSCC cell lines in EGFR after being conditioned by VCAF-I-582 CM compared to all the other conditions quite clearly. There are studies that link increased invasiveness of breast cancer and increased EGFR (Ohnishi et al., 2014; Xing & Fadare, 2021), meaning that EGFR could be the sole, but more likely could be a part of a plethora of proteins that are either inhibited or higher expressed directly or indirectly by the miR-582-5p which causes this phenotype. Also, there is a minor increase in expression of YAP in the UMSCV4 E6E7 cell lines after being conditioned by VCAF-I-582 CM. . Although both EGFR and YAP (Dupont et al., 2011; Zhu et al., 2021) have been involved in increasing invasiveness in many carcinomas, these observations needs to be validated with further experiments to give insight into the underlying mechanism.

Refrences

Costea, D. E., Hills, A., Osman, A. H., Thurlow, J., Kalna, G., Huang, X., Pena Murillo, C., Parajuli, H., Suliman, S., Kulasekara, K. K., Johannessen, A. C., & Partridge, M. (2013). Identification of two distinct carcinoma-associated fibroblast subtypes with differential tumor-promoting abilities in oral squamous cell carcinoma. *Cancer Res*, *73*(13), 3888-3901. https://doi.org/10.1158/0008-5472.Can-12-4150

Croce, C. M. (2009). Causes and consequences of microRNA dysregulation in cancer. *Nature Reviews Genetics*, *10*(10), 704-714. https://doi.org/10.1038/nrg2634

D'Arcangelo, E., Wu, N. C., Cadavid, J. L., & McGuigan, A. P. (2020). The life cycle of cancer-associated fibroblasts within the tumour stroma and its importance in disease outcome. *British Journal of Cancer*, *122*(7), 931-942. https://doi.org/10.1038/s41416-019-0705-1

Dauer, P., Zhao, X., Gupta, V. K., Sharma, N., Kesh, K., Gnamlin, P., Dudeja, V., Vickers, S. M., Banerjee, S., & Saluja, A. (2018). Inactivation of Cancer-Associated-Fibroblasts Disrupts Oncogenic Signaling in Pancreatic Cancer Cells and Promotes Its Regression. *Cancer research*, *78*(5), 1321-1333. https://doi.org/10.1158/0008-5472.CAN-17-2320

Dongre, H., Rana, N., Fromreide, S., Rajthala, S., Bøe Engelsen, I., Paradis, J., Gutkind, J. S., Vintermyr, O. K., Johannessen, A. C., Bjørge, L., & Costea, D. E. (2020). Establishment of a novel cancer cell line derived from vulvar carcinoma associated with lichen sclerosus exhibiting a fibroblast-dependent tumorigenic potential. *Experimental Cell Research*, *386*(1), 111684. https://doi.org/https://doi.org/10.1016/j.yexcr.2019.111684

Dongre, H., Rana, N., Fromreide, S., Rajthala, S., Engelsen, I., Paradis, J., Gutkind, J. S., Vintermyr, O., Johannessen, A., Bjørge, L., & Costea, D. (2019). Establishment of a novel cancer cell line derived from vulvar carcinoma associated with lichen sclerosus exhibiting a fibroblast-dependent tumorigenic potential. *Experimental Cell Research*, *386*, 111684. https://doi.org/10.1016/j.yexcr.2019.111684

Dupont, S., Morsut, L., Aragona, M., Enzo, E., Giulitti, S., Cordenonsi, M., Zanconato, F., Le Digabel, J., Forcato, M., Bicciato, S., Elvassore, N., & Piccolo, S. (2011). Role of YAP/TAZ in mechanotransduction. *Nature*, *474*(7350), 179-183. https://doi.org/10.1038/nature10137

Dvorak, H. F. (1986). Tumors: wounds that do not heal. Similarities between tumor stroma generation and wound healing. *N Engl J Med*, *315*(26), 1650-1659. https://doi.org/10.1056/nejm198612253152606

Hu, D., Zhou, J., Wang, F., Shi, H., Li, Y., & Li, B. (2015). HPV-16 E6/E7 promotes cell migration and invasion in cervical cancer via regulating cadherin switch in vitro and in vivo. *Archives of Gynecology and Obstetrics*, *292*(6), 1345-1354. https://doi.org/10.1007/s00404-015-3787-x

Iorio, M. V., & Croce, C. M. (2012). MicroRNA dysregulation in cancer: diagnostics, monitoring and therapeutics. A comprehensive review. *EMBO molecular medicine*, *4*(3), 143-159. https://doi.org/10.1002/emmm.201100209

Jin, M.-Z., & Jin, W.-L. (2020). The updated landscape of tumor microenvironment and drug repurposing. *Signal Transduction and Targeted Therapy*, *5*(1), 166. https://doi.org/10.1038/s41392-020-00280-x

Kendall, R. T., & Feghali-Bostwick, C. A. (2014). Fibroblasts in fibrosis: novel roles and mediators [Review]. *Frontiers in Pharmacology*, *5*. https://doi.org/10.3389/fphar.2014.00123

Kombe Kombe, A. J., Li, B., Zahid, A., Mengist, H. M., Bounda, G.-A., Zhou, Y., & Jin, T. (2021). Epidemiology and Burden of Human Papillomavirus and Related Diseases, Molecular Pathogenesis, and Vaccine Evaluation [Review]. *Frontiers in Public Health*, *8*. https://doi.org/10.3389/fpubh.2020.552028

Lemons, J. M. S., Feng, X.-J., Bennett, B. D., Legesse-Miller, A., Johnson, E. L., Raitman, I., Pollina, E. A., Rabitz, H. A., Rabinowitz, J. D., & Coller, H. A. (2010). Quiescent fibroblasts exhibit high metabolic activity. *PLoS biology*, *8*(10), e1000514-e1000514. https://doi.org/10.1371/journal.pbio.1000514

Lindell, G., Näsman, A., Jonsson, C., Ehrsson, R. J., Jacobsson, H., Danielsson, K. G., Dalianis, T., Källström, B. N., & Larson, B. (2010). Presence of human papillomavirus (HPV) in vulvar squamous cell carcinoma (VSCC) and sentinel node. *Gynecol Oncol*, *117*(2), 312-316. https://doi.org/10.1016/j.ygyno.2009.12.031

Liu, L., Liu, L., Yao, H. H., Zhu, Z. Q., Ning, Z. L., & Huang, Q. (2016). Stromal Myofibroblasts Are Associated with Poor Prognosis in Solid Cancers: A Meta-Analysis of Published Studies. *PloS one*, *11*(7), e0159947-e0159947. https://doi.org/10.1371/journal.pone.0159947

Mantovani, A., Allavena, P., Sica, A., & Balkwill, F. (2008). Cancer-related inflammation. *Nature*, *454*(7203), 436-444. https://doi.org/10.1038/nature07205

Meltzer-Gunnes, C. J., Småstuen, M. C., Kristensen, G. B., Tropé, C. G., Lie, A. K., & Vistad, I. (2017). Vulvar carcinoma in Norway: A 50-year perspective on trends in incidence, treatment and survival. *Gynecologic Oncology*, *145*(3), 543-548. https://doi.org/https://doi.org/10.1016/j.ygyno.2017.03.008

Miranda, A., Hamilton Phineas, T., Zhang Allen, W., Pattnaik, S., Becht, E., Mezheyeuski, A., Bruun, J., Micke, P., de Reynies, A., & Nelson Brad, H. (2019). Cancer stemness, intratumoral heterogeneity, and immune response across cancers. *Proceedings of the National Academy of Sciences*, *116*(18), 9020-9029. https://doi.org/10.1073/pnas.1818210116

Müller, M., Hermann, P. C., Liebau, S., Weidgang, C., Seufferlein, T., Kleger, A., & Perkhofer, L. (2016). The role of pluripotency factors to drive stemness in gastrointestinal cancer. *Stem Cell Research*, *16*(2), 349-357. https://doi.org/https://doi.org/10.1016/j.scr.2016.02.005

Münger, K., Baldwin, A., Edwards Kirsten, M., Hayakawa, H., Nguyen Christine, L., Owens, M., Grace, M., & Huh, K. (2004). Mechanisms of Human Papillomavirus-Induced Oncogenesis. *Journal of Virology*, *78*(21), 11451-11460. https://doi.org/10.1128/JVI.78.21.11451-11460.2004

Ohnishi, Y., Watanabe, M., Yasui, H., & Kakudo, K. (2014). Effects of epidermal growth factor on the invasive activity and cytoskeleton of oral squamous cell

carcinoma cell lines. *Oncology letters*, *7*(5), 1439-1442. https://doi.org/10.3892/ol.2014.1946

Pal, M. K., Jaiswar, S. P., Dwivedi, V. N., Tripathi, A. K., Dwivedi, A., & Sankhwar, P. (2015). MicroRNA: a new and promising potential biomarker for diagnosis and prognosis of ovarian cancer. *Cancer Biol Med*, *12*(4), 328-341. https://doi.org/10.7497/j.issn.2095-3941.2015.0024

Peng, Y., & Croce, C. M. (2016). The role of MicroRNAs in human cancer. *Signal Transduction and Targeted Therapy*, *1*(1), 15004. https://doi.org/10.1038/sigtrans.2015.4

Place Robert, F., Li, L.-C., Pookot, D., Noonan Emily, J., & Dahiya, R. (2008). MicroRNA-373 induces expression of genes with complementary promoter sequences. *Proceedings of the National Academy of Sciences*, *105*(5), 1608-1613. https://doi.org/10.1073/pnas.0707594105

Puppo, V. (2013). Anatomy and physiology of the clitoris, vestibular bulbs, and labia minora with a review of the female orgasm and the prevention of female sexual dysfunction. *Clinical Anatomy*, *26*(1), 134-152. https://doi.org/https://doi.org/10.1002/ca.22177

Rajthala, S., Min, A., Parajuli, H., Debnath, K. C., Ljøkjel, B., Hoven, K. M., Kvalheim, A., Lybak, S., Neppelberg, E., Vintermyr, O. K., Johannessen, A. C., Sapkota, D., & Costea, D. E. (2021). Profiling and Functional Analysis of microRNA Deregulation in Cancer-Associated Fibroblasts in Oral Squamous Cell Carcinoma Depicts an Anti-Invasive Role of microRNA-204 via Regulation of Their Motility. *International journal of molecular sciences*, *22*(21), 11960. https://doi.org/10.3390/ijms222111960

Sahai, E., Astsaturov, I., Cukierman, E., DeNardo, D. G., Egeblad, M., Evans, R. M., Fearon, D., Greten, F. R., Hingorani, S. R., Hunter, T., Hynes, R. O., Jain, R. K., Janowitz, T., Jorgensen, C., Kimmelman, A. C., Kolonin, M. G., Maki, R. G., Powers, R. S., Puré, E., . . . Werb, Z. (2020). A framework for advancing our understanding of cancer-associated fibroblasts. *Nature Reviews Cancer*, *20*(3), 174-186. https://doi.org/10.1038/s41568-019-0238-1

Shah, F. D., Begum, R., Vajaria, B. N., Patel, K. R., Patel, J. B., Shukla, S. N., & Patel, P. S. (2011). A Review on Salivary Genomics and Proteomics Biomarkers in Oral Cancer. *Indian Journal of Clinical Biochemistry*, *26*(4), 326-334. https://doi.org/10.1007/s12291-011-0149-8

Shu, Z., Chen, L., & Ding, D. (2016). miR-582-5P induces colorectal cancer cell proliferation by targeting adenomatous polyposis coli. *World Journal of Surgical Oncology*, *14*(1), 239. https://doi.org/10.1186/s12957-016-0984-4

Todoric, J., & Karin, M. (2019). The Fire within: Cell-Autonomous Mechanisms in Inflammation-Driven Cancer. *Cancer Cell*, *35*(5), 714-720. https://doi.org/10.1016/j.ccell.2019.04.001

Tomaić, V. (2016). Functional Roles of E6 and E7 Oncoproteins in HPV-Induced Malignancies at Diverse Anatomical Sites. *Cancers*, *8*(10), 95. https://doi.org/10.3390/cancers8100095

Wang, X., Huang, X., & Zhang, Y. (2018). Involvement of Human Papillomaviruses in Cervical Cancer [Review]. *Frontiers in Microbiology*, *9*. https://doi.org/10.3389/fmicb.2018.02896

Xing, D., & Fadare, O. (2021). Molecular events in the pathogenesis of vulvar squamous cell carcinoma. *Seminars in diagnostic pathology*, *38*(1), 50-61. https://doi.org/10.1053/j.semdp.2020.09.010

Xu, N., Papagiannakopoulos, T., Pan, G., Thomson, J. A., & Kosik, K. S. (2009). MicroRNA-145 Regulates OCT4, SOX2, and KLF4 and Represses Pluripotency in Human Embryonic Stem Cells. *Cell*, *137*(4), 647-658. https://doi.org/https://doi.org/10.1016/j.cell.2009.02.038

Zhang, J., Zhang, Y., & Zhang, Z. (2018). Prevalence of human papillomavirus and its prognostic value in vulvar cancer: A systematic review and meta-analysis. *PloS one*, *13*(9), e0204162-e0204162. https://doi.org/10.1371/journal.pone.0204162

Zhu, B., V, M., Finch-Edmondson, M., Lee, Y., Wan, Y., Sudol, M., & DasGupta, R. (2021). miR-582-5p Is a Tumor Suppressor microRNA Targeting the Hippo-YAP/TAZ Signaling Pathway in Non-Small Cell Lung Cancer. *Cancers (Basel)*, *13*(4). https://doi.org/10.3390/cancers13040756

Öhlund, D., Elyada, E., & Tuveson, D. (2014). Fibroblast heterogeneity in the cancer wound. *The Journal of experimental medicine*, *211*(8), 1503-1523. https://doi.org/10.1084/jem.20140692